

1989

Observations of tides and tidal currents in Elkhorn Slough

Cary Randall Wong
San Jose State University

Follow this and additional works at: https://scholarworks.sjsu.edu/etd_theses

Recommended Citation

Wong, Cary Randall, "Observations of tides and tidal currents in Elkhorn Slough" (1989). *Master's Theses*. 3236.

DOI: <https://doi.org/10.31979/etd.6qsy-ztb9>

https://scholarworks.sjsu.edu/etd_theses/3236

This Thesis is brought to you for free and open access by the Master's Theses and Graduate Research at SJSU ScholarWorks. It has been accepted for inclusion in Master's Theses by an authorized administrator of SJSU ScholarWorks. For more information, please contact scholarworks@sjsu.edu.

INFORMATION TO USERS

The most advanced technology has been used to photograph and reproduce this manuscript from the microfilm master. UMI films the text directly from the original or copy submitted. Thus, some thesis and dissertation copies are in typewriter face, while others may be from any type of computer printer.

The quality of this reproduction is dependent upon the quality of the copy submitted. Broken or indistinct print, colored or poor quality illustrations and photographs, print bleedthrough, substandard margins, and improper alignment can adversely affect reproduction.

In the unlikely event that the author did not send UMI a complete manuscript and there are missing pages, these will be noted. Also, if unauthorized copyright material had to be removed, a note will indicate the deletion.

Oversize materials (e.g., maps, drawings, charts) are reproduced by sectioning the original, beginning at the upper left-hand corner and continuing from left to right in equal sections with small overlaps. Each original is also photographed in one exposure and is included in reduced form at the back of the book.

Photographs included in the original manuscript have been reproduced xerographically in this copy. Higher quality 6" x 9" black and white photographic prints are available for any photographs or illustrations appearing in this copy for an additional charge. Contact UMI directly to order.



University Microfilms International
A Bell & Howell Information Company
300 North Zeeb Road, Ann Arbor, MI 48106-1346 USA
313/761-4700 800/521-0600

Order Number 1339662

Observations of tides and tidal currents in Elkhorn Slough

Wong, Cary Randall, M.S.

San Jose State University, 1989

U·M·I
300 N. Zeeb Rd.
Ann Arbor, MI 48106

OBSERVATIONS OF TIDES AND
TIDAL CURRENTS IN ELKHORN SLOUGH

A Thesis
Presented to
The Faculty of Moss Landing Marine Laboratories

In Partial Fulfillment
of the Requirements for the Degree
Master of Science
in Marine Science

By
Cary Randall Wong
December 1989

APPROVED FOR MOSS LANDING MARINE LABORATORIES

William Broenkow

Dr. William W. Broenkow

Kenneth S. Johnson

Dr. Kenneth S. Johnson

Giacomo R. DiTullio

Dr. Giacomo R. DiTullio

APPROVED FOR THE UNIVERSITY

Serena H. Stanford

ABSTRACT

OBSERVATIONS OF TIDES AND TIDAL CURRENTS IN ELKHORN SLOUGH

by Cary R. Wong

Marshland restoration, from 1983 to 1986, has altered the hydrography of Elkhorn Slough. A time series study of tidal height and current velocity in September 1986 characterized the changed tidal regime.

Results indicate that intertidal water storage over the tidal flats was responsible for an asymmetric tide, a longer rising water duration and a higher ebb current. These characteristics classify Elkhorn Slough as an ebb dominant system. Tide asymmetry was also indicated by the generation of shallow water constituents, M4, MK3 and 2MK3.

Phase lags of high and low water have doubled since 1976, and at the slough entrance, currents have increased 55% since 1972. The highest predicted current velocity is now 113 cm/s. Low tide volume has increased from 2.0×10^6 to $2.1 \times 10^6 \text{ m}^3$ while diurnal high tide volume has increased from 6.0×10^6 to $7.8 \times 10^6 \text{ m}^3$ with a mean diurnal tidal prism of $5.7 \times 10^6 \text{ m}^3$.

ACKNOWLEDGEMENTS

I am indebted to my research advisor, Dr. William W. Broenkow, for his continued assistance and support. I express my gratitude to my other committee members, Dr. Kenneth S. Johnson and Dr. Giacomo R. DiTullio for their critical comments and suggestions.

I appreciate the efforts and technical expertise provided by Mark Yarbrough and computer programming assistance rendered by Richard Reaves.

I thank the many students of Moss Landing Marine Laboratories, who contributed their efforts to this project. Most notable are Andrew Heard for his dependable presence in the field and Marilyn Yuen for her valuable comments and moral support.

I wish to recognize Mark Silberstein, for his enthusiasm and support during the initiation of this project.

Most of all, I wish to express my deepest appreciation to my wife for her continued support and endless patience.

This research was supported by NOAA grant NA86AA-D-CZ033.

TABLE OF CONTENTS

	PAGE
ABSTRACT	iii
INTRODUCTION	1
Oceanographic Background	4
Equilibrium Tide	4
Tidal Constituents	7
Ocean and Shallow Water Tides	11
Tidal Currents	17
Geology	17
Recorded History	18
Previous Studies	21
Purpose of Study	23
METHODS	25
Instrumentation	25
Pressure	25
Field Work	26
Data Processing	32
Pressure Correction	33
Comparison of Endeco and S4 Current Meters	35
Vertical Profiling	39
RESULTS AND DISCUSSION	41
Tidal Elevation	41
Duration of Rising and Falling Water Level	48
Phase Lags	56

Temperature	57
Tidal Currents	64
Effective Surface Area and Volume Transport	85
CONCLUSIONS	95
REFERENCES	98
APPENDIX 1. Current meter characteristics and calibration	102
APPENDIX 2. Tidal Constituents	105

LIST OF TABLES

<u>Table</u>	<u>Page</u>
1. Astronomical elements of a tide constituent argument	9
2. Classification of tides based on the local response to diurnal and semidiurnal constituents	9
3. Variances of tidal elevation of the four largest tidal periods, derived from spectral analysis ...	44
4. Mean duration of rising and falling water	47
5. The primary astronomical and shallow water constituents used to model tide asymmetry in Elkhorn Slough, based on NOAA station # 493 tide constituents	54
6. Phase lag of high and Low water relative to Monterey predicted tides, during September 1986 .	57
7. Observed water temperature during September 1986.	58
8. Phase lag and variance between the time of highest tide height and time of highest water temperature for the semidiurnal period, derived from cross spectral analysis	61
9. Maximum observed current velocities during September 1986	72
10. Mean duration of rising and falling water and mean lag to maximum current velocity, during September 1986	76
11. Statistics of least squares regression of maximum current velocity vs H/T for stations 1, 2, 3 and Clark's (1972) station	80
12. Cumulative surface area and volume estimates, derived from maximum current velocity observations	86
13. Statistics of least squares regression of exchange volume vs tidal range for stations 1, 2 and 3, based on the integral method	90

<u>Table</u>	<u>Page</u>
14. Exchange volume calculated by the integrated volume transport method	91
15. Cumulative surface area of South Marsh and Parson Slough, derived from planimetered data ...	92
16. Volume estimate of South Marsh and Parson Slough, derived from planimetered cumulative surface areas	92

LIST OF FIGURES

<u>Figure</u>	<u>Page</u>
1. Chart of Monterey Bay and Elkhorn Slough	2
2. Difference in the moon's gravitational attraction, $F_m = GMm / (P \pm R)^2$, on water parcels at different points, a and b, on the earth	5
3. Hourly phase of semidiurnal cotidal lines extending from an amphidromic point in the Northeastern Pacific Ocean	12
4. Tide asymmetry resulting from shallow water tidal wave propagation	15
5. General physical features and commercial operations at the entrance to Elkhorn Slough	19
6. Idealized cross section of Elkhorn Slough	22
7. Map of Elkhorn Slough and station sites	27
8. Cross channel profiles at stations where current velocity observations were taken	28
9. Current meter mooring configuration	30
10. Correlation between uncorrected pressure transducer tidal height with uncorrected tide staff tidal height	36
11. A) Comparison of Endeco and S4 current velocities at station 1. B) Closeup showing a major Endeco fouling period. C) Correlation between Endeco and S4 current velocities	37
12. A) Comparison of water temperature between Endeco and S4 meters at station 1. B) Correlation between Endeco and S4 temperature .	38
13. Time series of corrected observed tides at stations shown in Fig. 7	42
14. Tidal height spectra at stations in Fig. 7	43

<u>Figure</u>	<u>Page</u>
15. Comparison of relative tide staff heights with Monterey Bay predicted tides (based on NOAA constituents). A) slough entrance B) South Marsh .	46
16. Duration of rising and falling water at stations shown in Fig. 7	49
17. Model of tide asymmetry produced by different phasing of M_2 and M_4 constituents. M_4/M_2 amplitude ratio = 0.3. A) phase = 0° B) phase = 90° C) phase = 180° D) phase = 270°	52
18. Duration and the difference in duration of the predicted tides using the (K_1 M_2) and (K_1 M_2 M_4 MK_3 $2MK_3$) tidal constituents (based on 1976 NOAA station # 493 tide constituents)	55
19. Time series of observed water temperature at stations shown in Fig. 7	59
20. Water temperature spectra showing large diurnal and semidiurnal variances at stations 1 through 3, but only large diurnal variance at station	60
21. Correlation between the daily solar irradiance and daily mean water temperature. A) Correlation with no lag. B) Correlation with solar irradiance lagged one day. C) Correlation between potential thermal heating with daily mean water temperature.	63
22. Time series of observed current velocity at stations shown in Fig. 7	65
23. Time series of observed cross-channel current velocity at stations shown in Fig. 7	66
24. Vertical current velocity distributions from the bottom to the surface, at station 1. Vertical profiles observed at peak current flow	68
25. Determining roughness length, Z_0 , within the boundary layer, at station 1	69
26. Comparison of the average velocity defect observed at station 1 with the theoretical velocity defect distribution	70

<u>Figure</u>	<u>Page</u>
27. Current velocity spectra for stations shown in Fig. 7	74
28. Current and tidal elevation at station 2 on 15 September 1986. Note that the time of maximum flood current velocity is shifted towards the time of high tide	77
29. Least squares regression of maximum current with tide height rate of change, at stations shown in Fig. 7 and Clark's (1972) Highway 1 Bridge station	79
30. Least squares regression of exchange volume with tidal range at stations shown in Fig. 7	89
31. Aerial photograph of Elkhorn Slough, at low tide on 19 May 1983. Scale = 1:24000	93

INTRODUCTION

Coastal regions, such as Elkhorn Slough and San Francisco Bay, have been highly modified by the influence of man. Early land usage focused on the development of estuarine environments and the consequent removal of wetlands from tidal circulation. After many years of reclaiming marshland from tidal influence, a growing awareness of the damage done to the environment caused a slow down, and in Elkhorn Slough, a reversal in the practice of diking tidal lands. The effect on the slough's hydrography of restoring former salt marshes back to tidal influence, is investigated in this study.

Elkhorn Slough is a shallow tidal embayment located at the head of Monterey Bay, California (Fig. 1). During most of the year, the combination of negligible freshwater input and evaporation produces hypersaline conditions typically found in coastal lagoons, such as along the Gulf Coast of southern Texas. Although the slough does not exhibit estuarine conditions throughout the majority of the year, it is often referred to as an estuary.

Early use of both Elkhorn Slough and San Francisco Bay encompassed considerable wetland reclamation. Since the mid 1800's wetlands have been reclaimed for urban, industrial and agricultural use in the San Francisco bay system and for agricultural use in slough. Organized

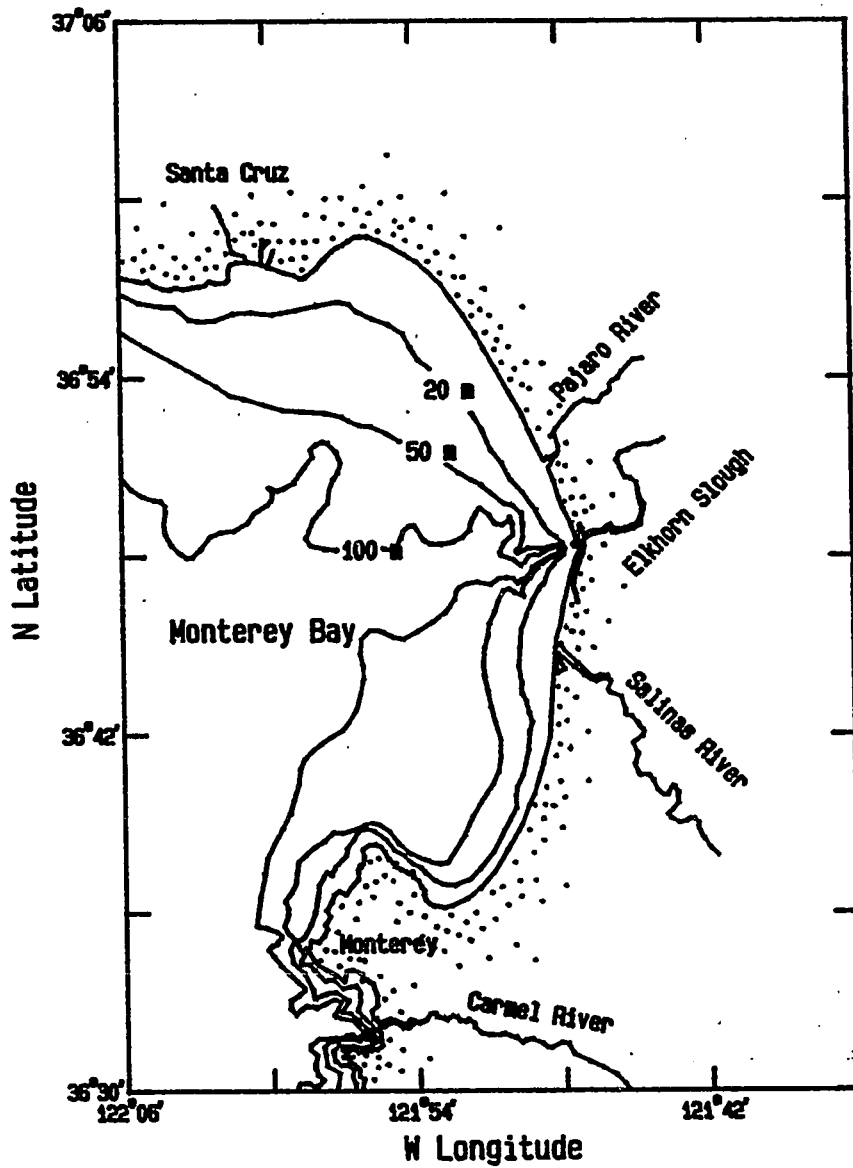


Figure 1. Chart of Monterey Bay and Elkhorn Slough.

efforts to maintain tidal marshes in their pristine condition began only after the 1960's, in California. Ecological concern over the extensive loss of California's coastal wetlands has led to the creation of organizations such as the San Francisco Bay Conservation and Development Commission (BCDC), the Nature Conservancy and Elkhorn Slough National Estuarine Research Reserve (ESNERR). The main impetus of the BCDC has been to preserve the remaining tidal marshes in and around San Francisco Bay.

The ESNERR has actively restored former marshland to tidal circulation. In 1983, and again in 1985, several hundred acres of former wetlands were intentionally returned to tidal influence as part of ESNERR management. This acreage, along with marshlands restored to tidal circulation resulting from dike failures, has significantly increased the area subjected to tidal circulation and the water volume of the slough.

Presumably, the recent addition of tidally influenced wetlands to the slough system has modified its hydrography. The California Department of Fish and Game, which administers the ESNERR, has plans to enhance and restore other wetland areas within the slough. The information presented here is intended to be useful for formulating plans for the future of Elkhorn Slough, since understanding the physical processes is an important aspect of effective management planning.

Oceanographic Background

Open ocean tides drive the vertical and horizontal motion of water in Elkhorn Slough. As such, a brief discussion of tidal theory is presented as background for this study.

Equilibrium Tide. Tides are caused by the difference in gravitational forces resulting from the change of position of the sun and moon relative to points on the earth's surface. The force of gravity is proportional to the product of the masses of the two objects and inversely proportional to the square of the distance between them (Knauss, 1978).

Consider the gravitational attraction between the moon and water parcels at two points, a and b, on the earth's surface (Fig. 2). The gravitational attraction and the centripetal acceleration of the earth-moon system are in dynamic balance with respect to the common axis of rotation. Although centrifugal force, F_c , is the same for all points on the earth, a slight difference in the moon's gravitational attraction is exerted on parcels of water on the earth's surface by:

$$F_m = GMm / (P \pm R)^2, \quad (1)$$

where F_m is the moon's gravitational attraction, G is the universal gravitation constant, M is the mass of the moon, m is the mass of a water parcel on the surface of the

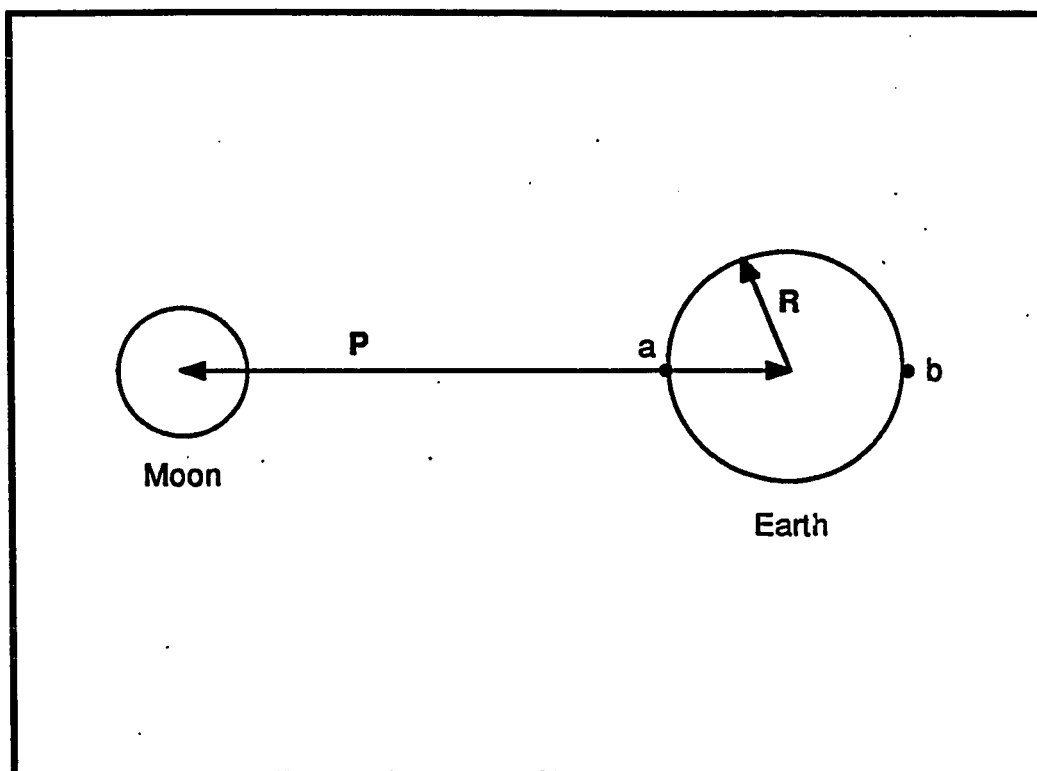


Figure 2. Difference in the moon's gravitational attraction, $F_m = GMm / (P \pm R)^2$, on water parcels at different points, a and b, on the earth.

earth, P is the distance between the center of the earth and moon, and R is the earth's radius. The deviation in F_m is about 3% greater at point a, and 3% less at point b, relative to the center of the earth. A larger value of F_m on the sublunar side of the earth causes a net gravitational attraction directed towards the moon and a smaller value on the side opposite the moon causes a net centrifugal force directed outward from the moon. The differential force $F_m - F_c$, is proportional to M/P^3 , and is the force responsible for the creation of tides (Knauss, 1978).

The differential force can be resolved into vertical and horizontal components. The maximum vertical components located at points closest to and opposite the moon are seven orders of magnitude less than the earth's gravity and is usually disregarded (Pond and Pickard, 1983). The horizontal component or tractive force is also small, but is comparable to other barotropic and baroclinic pressure forces in the ocean. The tractive force is the effective force responsible for tidal generation.

In equilibrium theory, the entire earth is considered to be covered with water of uniform depth and density and the effects of friction are omitted. The envelope of water surrounding the earth would form two bulges in accordance to the tractive force. With the earth rotating beneath the mounds of water, a point on the surface of the earth would

experience two high and two low stands of water during each lunar day. The rotation of the earth about its axis beneath two mounds of water generated from the tractive force of the moon is the principle behind the semidiurnal tide.

The same principle describing the lunar tide-generating force is also true for the sun. The influence of tide-generating force for the earth/sun system is independent of the earth/moon system and the resultant tide is the summation of all the tide-generating forces.

Tidal Constituents. In principle, all astronomical bodies in the universe produce tide-generating forces. However, the next largest astronomical tide-generating body after the moon and sun is Venus, with a tractive force five orders of magnitude less than that of the moon. In reality, only the moon and sun are close enough to the earth with sufficient mass to significantly effect earth tides.

Other important astronomical components that contribute significantly to the height of the tide include: the elliptical orbits of the earth around the sun, the moon around the earth, and the variations in declination of the moon and sun with respect to the earth. Because the periods of astronomical components are precisely known, the resultant tide can be calculated as the sum of the amplitudes attributed to each tide-generating component

(i.e. constituent). The sum of all tide-generating components can be expressed as a simple harmonic equation (Schureman, 1971):

$$H_t = H_0 + \sum_{i=1}^{i=63} A_i * \cos (N_i * t - L_i), \quad (2)$$

where H_t is the tidal height at a given location, H_0 is the mean lower low water (MLLW) level at a given location where the tide datum is MLLW, A_i is the amplitude of the i th constituent, N_i is its speed number usually expressed in degrees/hour. Time, t , is usually reckoned from the beginning of the year, and L_i is the phase lag of the i th constituent between the time of maximum tide-generating force and the time of maximum local effect.

The coefficients in (2) are considered to be constant over a long period at a particular locality provided that there are no physical changes in the region that might affect the tidal conditions. The coefficient H_0 is the MLLW datum calculated from the arithmetic mean of the lower low water heights of a mixed tide observed over a 19 year metonic cycle. A_i is the maximum vertical displacement attributed to the i th constituent and is derived by harmonic analysis from observed data. N_i is the speed of the i th constituent and is formulated from angular constants and integer multiples of one or more of the four astronomical elements stated in Table 1 (Schureman, 1971). L_i is the interval between high water of an equilibrium

Table 1. Astronomical elements of a tide constituent
Argument (after Schureman, 1971).

Element	Speed (deg/hr)	Description
T	15.000000	mean solar day
s	0.549017	sidereal month relative to the fixed stars
h	0.410686	mean solar year
p	0.004642	revolution of lunar perigee

Table 2. Classification of tides based on the local
response to diurnal and semidiurnal
constituents.

Type	Tide description per lunar day
Diurnal	One high and one low water.
Semidiurnal	Two high and two low waters of about equal height.
Mixed, mainly Diurnal	Usually one high and one low with periods of two high and low waters of large inequalities in height and phase.
Mixed, mainly Semidiurnal	Two high and two low waters of large inequalities in height and phase.

tide to the high water of the local observed tide of the
ith constituent, derived from observed tides.

Up to 63 constituents are recognized as significant in
describing tides, although the four primary constituents
(K₁, O₁, M₂, S₂) can account for about 70% of the total
tidal amplitude (Defant, 1964). These constituents are
generally divided into three "species," with periods of
about half a day (semidiurnal), a day (diurnal) and long

period (periods of two weeks and longer).

Along the coast, there is considerable variability in the vertical displacement of tides based on the differences in the local response to the various constituents (Pond and Pickard, 1983). The different tide types are classified into four classes (Table 2): diurnal, common in the Gulf of Mexico; semidiurnal, typical along the U.S. Atlantic coast; mixed mainly diurnal, found in Manila; and mixed mainly semidiurnal, typical along the U.S. Pacific coast including Monterey Bay and Elkhorn Slough.

The amplitude and period of the tide along the Atlantic coast is regulated predominantly by the lunar semidiurnal constituent, M_2 , whereas on the Pacific coast, the mixed semidiurnal tide is influenced by both diurnal and semidiurnal constituents, K_1 and M_2 .

The four primary tidal constituents are used to systematically classify local tides into their tide types by the "form ratio," F , (Defant, 1964):

$$F = (K_1 + O_1) / (M_2 + S_2),$$

where K_1 , O_1 , M_2 and S_2 are the local tidal amplitudes of the lunisolar diurnal, principal lunar diurnal, principal lunar semidiurnal and principal solar semidiurnal constituents, respectively. Form ratios between 0 to 0.25 indicate equal semidiurnal tides, between 0.25 to 1.5, mixed mainly semidiurnal tides, between 1.5 to 3.0, mixed

mainly diurnal tides and greater than 3.0, diurnal tides. The form ratio of 0.96 for Monterey Bay is indicative of mixed semidiurnal tides.

Tide predictions are made by summing constituents with the most significant amplitudes into (2). Real tides vary from place to place due to local conditions. As a consequence, tide predictions are estimated empirically from observations of tidal height (taken for a minimum of 29 days) and the resultant tidal curve is analyzed to determine the amplitude and phasing of the harmonic constituents. These constituents are in turn reapplied to make future tide predictions.

Ocean and Shallow Water Tides. In the real ocean, equilibrium theory is modified by continent-bounded ocean basins of variable depth. Instead of tidal envelopes revolving around the earth, tidal waves propagate in rotary motion about nodal points within ocean basins. Nodes or amphidromic points are areas of vertically stationary sea level. Tidal waves extend out from each amphidromic point as lines of equal tidal phase, called cotidal lines (Fig. 3). In the northern hemisphere cotidal lines usually rotate in anti-clockwise direction.

In the Northeast Pacific Ocean, the oceanic tide progresses northward along the California coast until it enters into Monterey Bay and Elkhorn Slough. As the open ocean tidal wave reaches the relatively shallow water of

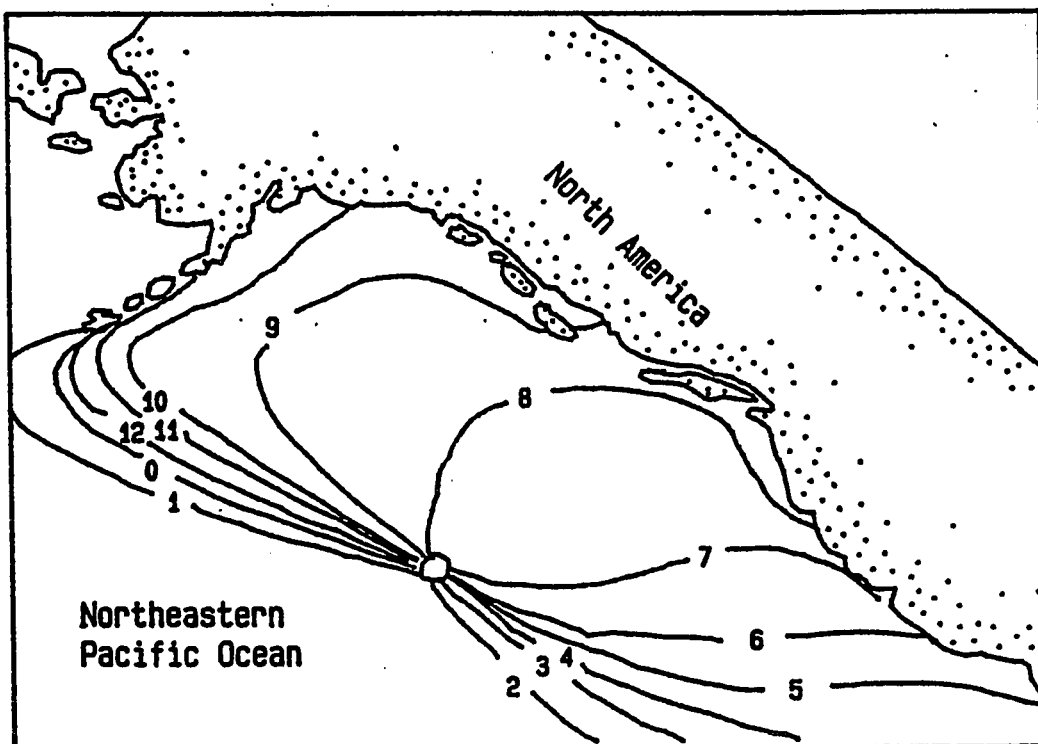


Figure 3. Hourly phase of semidiurnal cotidal lines extending from an amphidromic point in the Northeastern Pacific Ocean, from Defant (1974).

Monterey Bay and Elkhorn Slough its speed decreases while its height increases.

A tidal wave is a long period wave and its speed of propagation can be calculated by the Ideal Wave equation:

$$C = [gL/2\pi * \tanh(2\pi h/L)]^{1/2},$$

where C is wave celerity, g is gravitational coefficient (9.8 m/s^2), L is wavelength and h is water depth. When the ratio h/L is less than $1/20$, as in the case of tidal waves, the hyperbolic tangent function approaches one and celerity of shallow water waves can be approximated by:

$$C = [g(h+\zeta)]^{1/2}. \quad (3)$$

where ζ is tidal elevation.

Tidal waves entering a relatively shallow embayment or estuary will progress up the channel as a progressive wave. The progressive wave travels up the channel until it reaches the end, which acts as a barrier, where it may be reflected and travel as a progressive wave in the opposite direction back out into the open ocean. Providing that friction does not dampen out the progressive waves, a wave with standing wave characteristics may be created (Defant, 1964; Redfield, 1980).

The celerity of a shallow water wave can affect the phase velocity of the tide when the tidal amplitude becomes a significant fraction of the water depth. In the open

ocean, the period of a semidiurnal tide is 12.4 hr, with corresponding periods of rising and falling water equal to 6.2 hr. In an estuary, the duration of rising and falling water may become asymmetric when the tidal amplitude becomes a large fraction of the water depth. As water height varies over the tidal cycle, depth may be significantly greater at wave crest (high water) than at the wave trough (low water). Because the crest moves faster than the trough (3), high tide partially overtakes low tide and the tidal curve becomes distorted, such that the duration of rising tide is shorter than the duration of falling tide (Fig. 4) (Doodson and Warburg, 1952; Defant, 1964; Redfield, 1980). This process produces what has been termed a "flood dominant" system (Friedrichs and Aubrey, 1988). A "flood dominant" system is a tidal system that experiences a shorter interval of rising water than falling water and higher flood velocity than ebb velocity.

Friction reduces tidal amplitude and increases tidal phase lag in tidal embayments. Dissipation of tidal energy and increased phase lags are largest where channels are shallow (Aubrey and Speer, 1985). Thus, greater frictional effect retards the rate of water level change at low tide more than at high tide. Corresponding phase lags are longer at low tide than high tide resulting in longer durations of ebbing flow than flooding flow. Tidal wave asymmetry is enhanced in favor of a flood dominant system

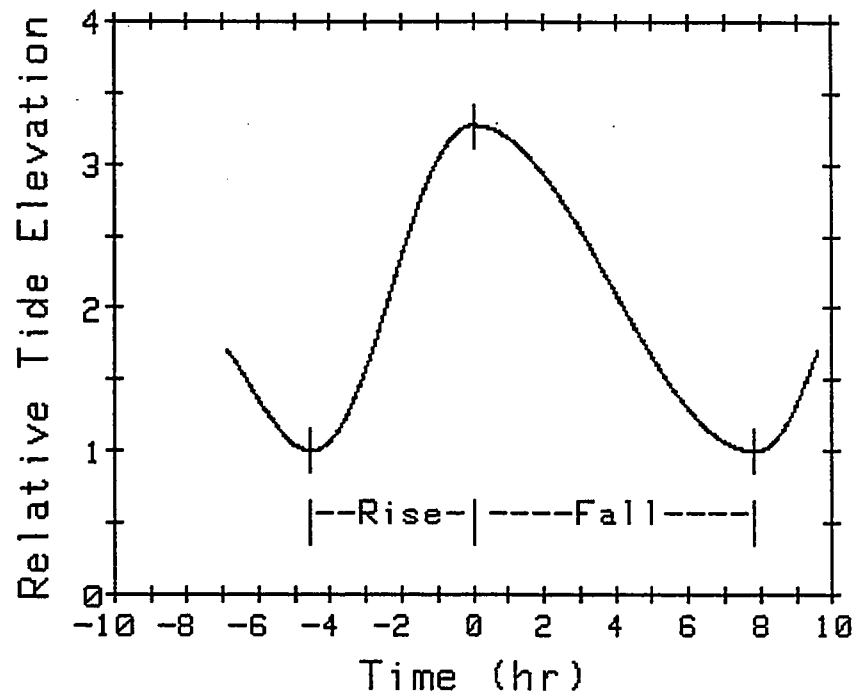


Figure 4. Tide asymmetry resulting from shallow water tidal wave propagation.

as the ratio of the tidal amplitude to tidal height or distance into an estuary increases.

"Ebb dominant" systems are tidal systems with a long duration of rising water and high ebb current velocity. Ebb dominance occurs in tidal systems that have a large ratio of intertidal storage volume to channel volume. Friction over intertidal marshes and flats can cause high tide to propagate slower than low tide, causing ebb tide to be short in duration and high in current velocity (Speer and Aubrey, 1985; Friedrichs and Aubrey, 1988).

Asymmetry in the rise and fall time of estuarine tides can be represented by the generation of higher order harmonics of the principal astronomic tide constituents (Boon and Byrne, 1981; Speer and Aubrey, 1985). Studies of asymmetric tidal propagation in estuaries along the U.S. east coast have shown that the relatively large magnitude of the M_2 constituent and its corresponding first harmonic overtide, M_4 , are the primary constituents regulating asymmetric tidal propagation there (Speer and Aubrey, 1985; Friedrichs and Aubrey, 1988). Numerical modelling (Boon and Byrne, 1981) has demonstrated that estuarine tide asymmetry can be traced to phase difference in the significant shallow water constituent relative to its predominant astronomical constituent. The asymmetric tide found in tidally influenced systems and its representation in the generation of higher order harmonics of the

principal astronomic constituents are important points which will be discussed later.

Tidal Currents. Tidal currents in narrow coastal inlets and channels, such as Elkhorn Slough, are reversing currents. A flood current flows inland during the rising tide and an ebb current flows seaward during the falling tide. The direction of current flow is generally parallel to the along-channel axis.

Since an incoming progressive wave and an outgoing reflected progressive wave can produce a wave with standing wave characteristics in tidal embayments, the time of maximum current flow generally occurs about midway between high and low tide. Slack water usually occurs around the time of highest and lowest water. Because large volumes of water may be transported through relatively narrow coastal inlets and straits, high tidal current velocities can occur within these tidal channels.

Geology

Elkhorn Slough has evolved through geological time and although the slough is a small geographic feature, its geologic history is linked to one of the world's largest submarine canyons. Elkhorn Valley was formed about the same time that the Monterey Submarine Canyon was formed during the late Pliocene and early Pleistocene (Martin, 1964). It has been suggested (Martin, 1964; Jenkins, 1974)

that periods of large scale drainage from the Santa Clara valley emptied into Monterey Bay through Elkhorn Slough. During the most recent low stand of sea level, 16,000 to 18,000 years ago, Elkhorn Slough was incised by river erosion to 30 m below present sea level. By the middle to late Pleistocene, tectonic activity along the San Andreas fault had disrupted most drainage through Elkhorn Valley (Schwartz, 1983). Between 8,000 and 10,000 years ago rising sea level produced a high energy tidal inlet similar to present day Elkhorn Slough. From 2,000 years ago to as recent as 1946, "extremely quiet estuarine conditions" existed in the slough allowing almost complete infilling of the slough (Schwartz, 1983).

Recorded History

Since recorded history Elkhorn Slough and the surrounding regions have been influenced by both natural and human factors. In the 1800's, the slough was a quiet shallow brackish water inlet less than 1 m deep and 5 m wide (MacGinitie, 1935). The mouth of the slough opened into the Salinas river which emptied into Monterey Bay just north of the slough, at the north end of Moss Landing Harbor (Fig. 5). Tidal exchange was highly restricted within the slough.

In the mid 1800's through the early 1900's much of the slough's wetlands were diked, ditched and drained for

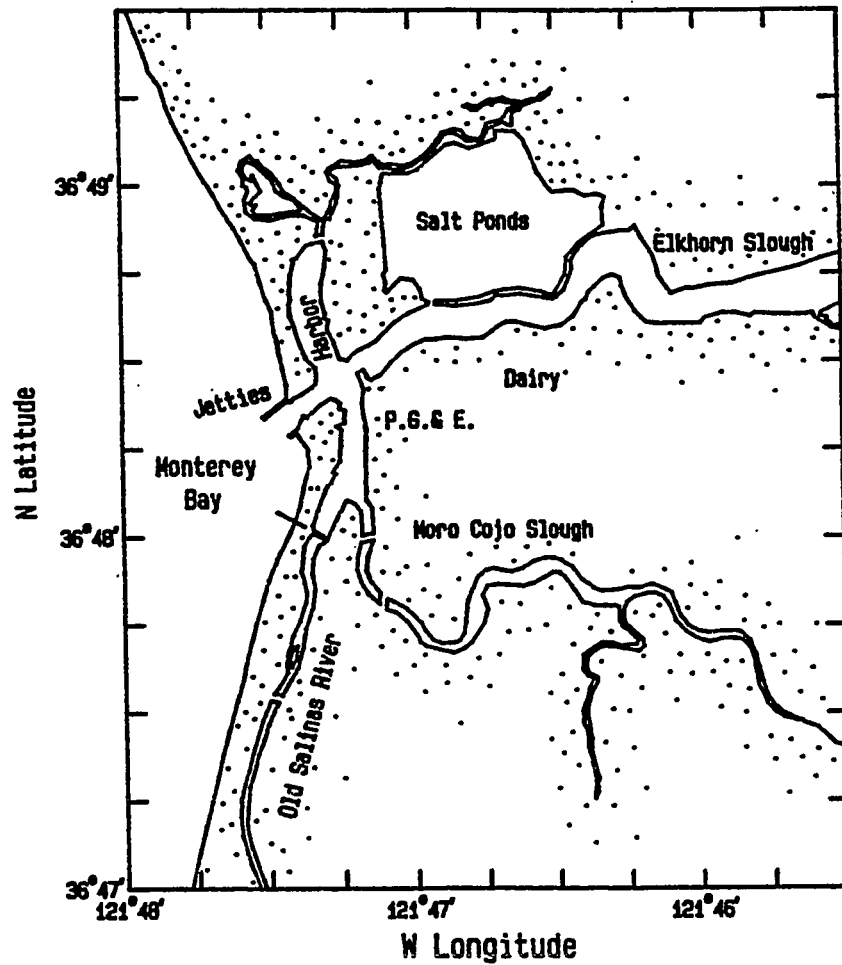


Figure 5. General physical features and commercial operations at the entrance to Elkhorn Slough.

agriculture (Gordon, 1977). A major change in the slough's hydrography during this reclamation period (1910) was the diversion of the Salinas River mouth into Monterey Bay, 8 km south of Elkhorn Slough (Fig. 1). This diversion removed a major source of freshwater, and it's likely that if the slough were left in this condition it would probably have evolved into a dry alluvial valley similar to other sloughs in the region (Schwartz, 1983).

The next major change in the slough's hydrography occurred in 1946 when the Moss Landing Harbor was completed. A permanent harbor entrance to Monterey Bay was opened in direct line with the slough's mouth (Fig. 5). The harbor entrance has had a dramatic effect on the slough's hydrography, changing it from a quiet shallow brackish water inlet with highly restricted tidal exchange into an expanding tidally influenced estuary with strong tidal currents.

Since the opening of the harbor entrance, several parcels of Elkhorn Slough (including South Marsh, Parson Slough, salt ponds, North Marsh and Dolan Marsh) have been restored to tidal inundation. Presently, Elkhorn Slough has an average channel depth of 3 m, ranging from 9 m at the entrance to 0.5 m near the head of the slough. Total length extends approximately 10 km inland and the average channel width is about 100 m. Extensive tidal flat, marshland and tidally restored land are present the length

of the slough channel. Although the slough contains over 12 km² of channel, tidal flat and salt marsh, the total drainage basin is only 585 km² (Browning, 1972).

The upper region is surrounded by agricultural lands, primarily artichoke and strawberry fields. The middle region is land controlled primarily by conservation groups, such as the Nature Conservancy and the ESNERR, which are interested in preserving the wetlands of the slough. Remnants of an oyster farm are visible along the north bank of the lower slough, which is adjacent to some salt ponds. Various private enterprises such as a dairy and the Pacific Gas and Electric (P.G. & E.) power plant are located along the south shore of the lower slough. The mouth of Elkhorn Slough splits the Moss Landing Harbor district where it intersects the Old Salinas River. Both Elkhorn Slough and the Old Salinas River channel have a common opening to Monterey Bay through a jetty that is in direct line with the entrance to the slough (Fig. 5).

Previous Studies

The oceanography and hydrography of Elkhorn Slough have been investigated by several researchers (Broenkow and Smith, 1972; Clark, 1972; Smith, 1974; Reilly, 1978). Clark's (1972) study, completed before restoration, indicated a maximum channel depth, at the Highway 1 bridge, of 7 m at high tide. Clark estimated that the effective

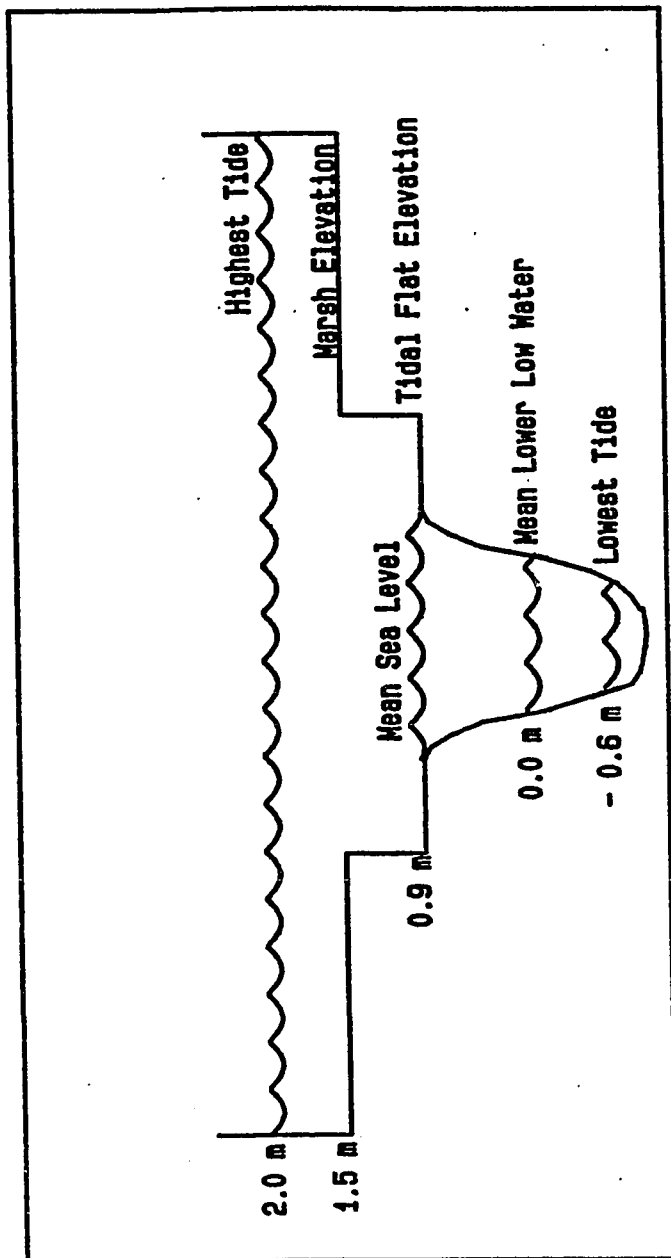


Figure 6. Idealized cross section of Elkhorn Slough, from Smith (1974).

slough area was 1.1 and 1.5 km², at low and high tide, respectively. He determined maximum current speeds at the entrance of the slough to be 60 and 70 cm/s for the flood and ebb tides.

Smith (1974) described the slough's cross sectional geometry as a three level system (Fig. 6). The lowest level is the slough channel, which is bordered by the tidal flats having an elevation of 0.9 m above MLLW and salt marshes at 1.5 m. From this idealized geometry of the slough he calculated the cumulative volume of Elkhorn Slough to be $6.0 \times 10^6 \text{ m}^3$ at high tide with a mean tidal prism of $4.0 \times 10^6 \text{ m}^3$. Smith also estimated tidal diffusion coefficients at various locations in the slough. The eddy diffusion coefficient ranged from $430 \times 10^4 \text{ cm}^2/\text{s}$, 2 km inland, to $5.9 \times 10^4 \text{ cm}^2/\text{s}$, 9 km inland. This led Smith to conclude that residence time in the upper slough to be in excess of 300 days.

Reilly (1974) found that flooding currents lasted longer and were lower in velocity than ebbing currents. In addition, he observed that tidal currents could be described using a 3-component harmonic regression that included the diurnal, semidiurnal and quarterdiurnal periods.

Purpose of Study

The primary objective of this study was to evaluate

the change in the hydrography of the slough system resulting from returning formerly diked wetlands to tidal circulation. Tidal height observations were used to establish the tidal range in the slough, durations of rising and falling water, and high and low tide phase lags from predicted Monterey Bay tides. Tidal heights were also compared to National Oceanic and Atmospheric Administration (NOAA) constituents, estimated in 1976, to determine changes in tide phase lags subsequent to the restoration.

Current velocity observations were compared to previous data to calculate changes in currents, caused by the addition of tidal lands, that coincided with increased tidal prism in the slough. Current and tidal data were used to establish the effective surface area, cumulative volume and tidal prism at selected locations of the slough over different tide elevations.

METHODS

Instrumentation

Five current meters were made available to this study from other Moss Landing Marine Laboratories (MLML) projects, during September 1986. Three of the meters were Endeco type 174 current meters and two were InterOcean Systems model S4 current meters. The Endeco is an axial-flow, ducted-impeller current meter. The S4 is a two axis electro-magnetic current meter.

The Endeco recording medium was digital magnetic tape. The sample interval was set to 2 min, and current speed, current direction, water temperature and pressure (tidal height) were digitized by an 8-bit A/D converter. Except for pressure measurements, calibrations for the Endeco meters were factory specified (Appendix 1).

The S4 meter recorded data internally in RAM memory modules. The sample interval was set to 2 min, and the S4 sampled voltage reference, northerly and easterly current vector components, water temperature and depth using 16-bit precision. All calibrations for the S4 meters were factory specified (Appendix 1):

Pressure

Tidal height was estimated using Kavlico P650 pressure transducers in the Endeco meters. Pressure calibrations

for the Kavlico P650 pressure transducers were performed at MLML using a 6 m standpipe filled with fresh water. Calibration curves estimating water depth were calculated directly from pressure counts (Appendix 1). Kavlico tidal height resolution was 0.5 cm with an accuracy of ± 2.5 cm. Full scale range was 11 m with a foldover range of 1.3 m.

Field Work

Five current meters were deployed at four stations in Elkhorn Slough from 12 through 29 September 1986 (Fig. 7). Station 1, located near the slough entrance, was established to monitor tidal heights and currents of lower Elkhorn Slough, and to estimate tidal flux of the slough as a whole. Station 2, located 4.5 km inland in a secondary channel leading to the South Marsh of the ESNERR and Parson Slough (SM/PS), was positioned to observe tidal heights and currents leading to SM/PS. This area was completely restored to tidal influence by 1984. Station 3, approximately 5 km inland in the main channel, was positioned to monitor tidal heights and currents affecting the upper slough. Station 4, located at the head of the South Marsh was established to examine tidal heights in the Research Reserve.

Current meters were deployed in the deepest area of the channel, determined by lead line soundings normal to the channel axis at each station (Fig 8). Tide staffs,

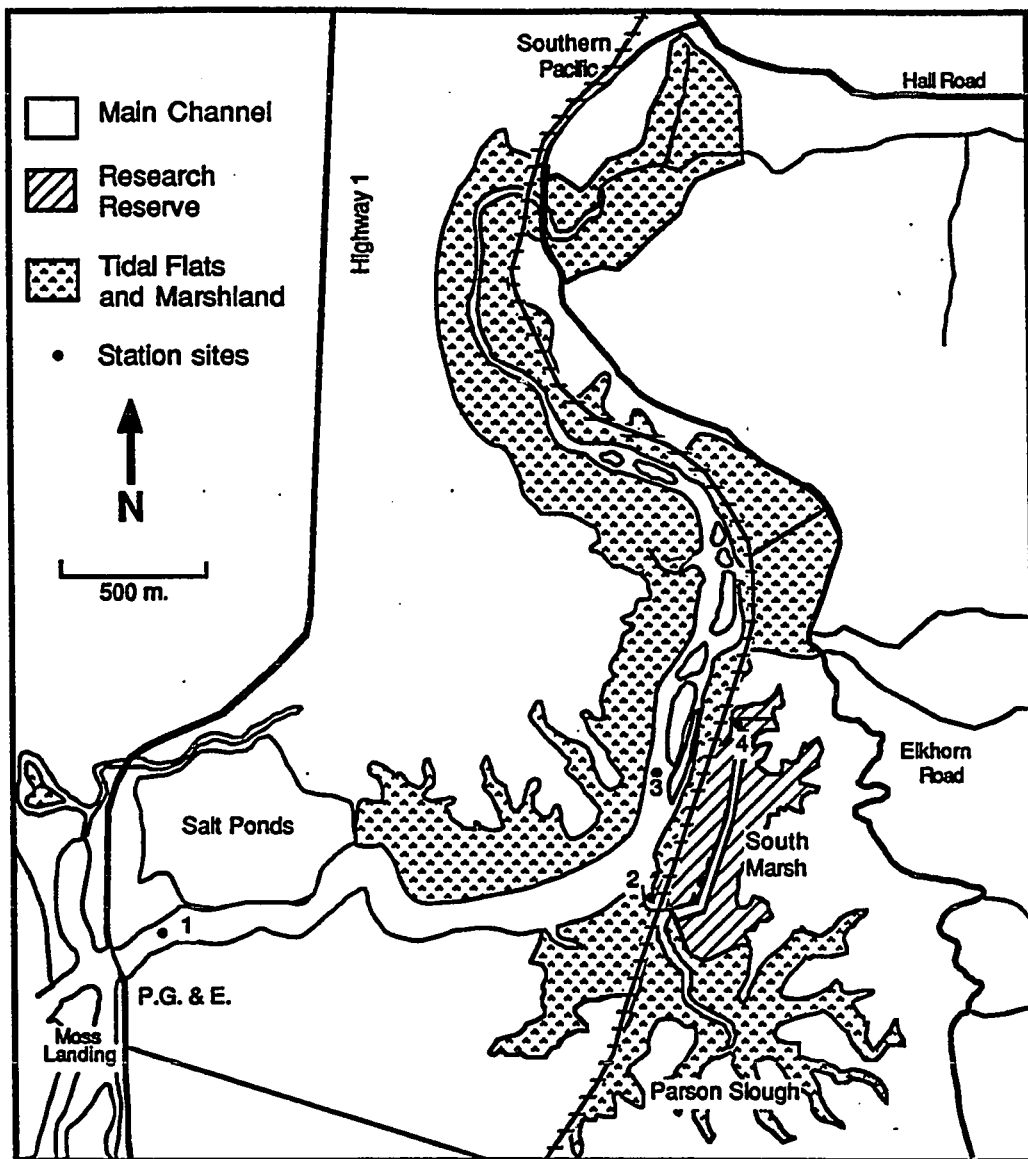


Figure 7. Map of Elkhorn Slough and station sites.

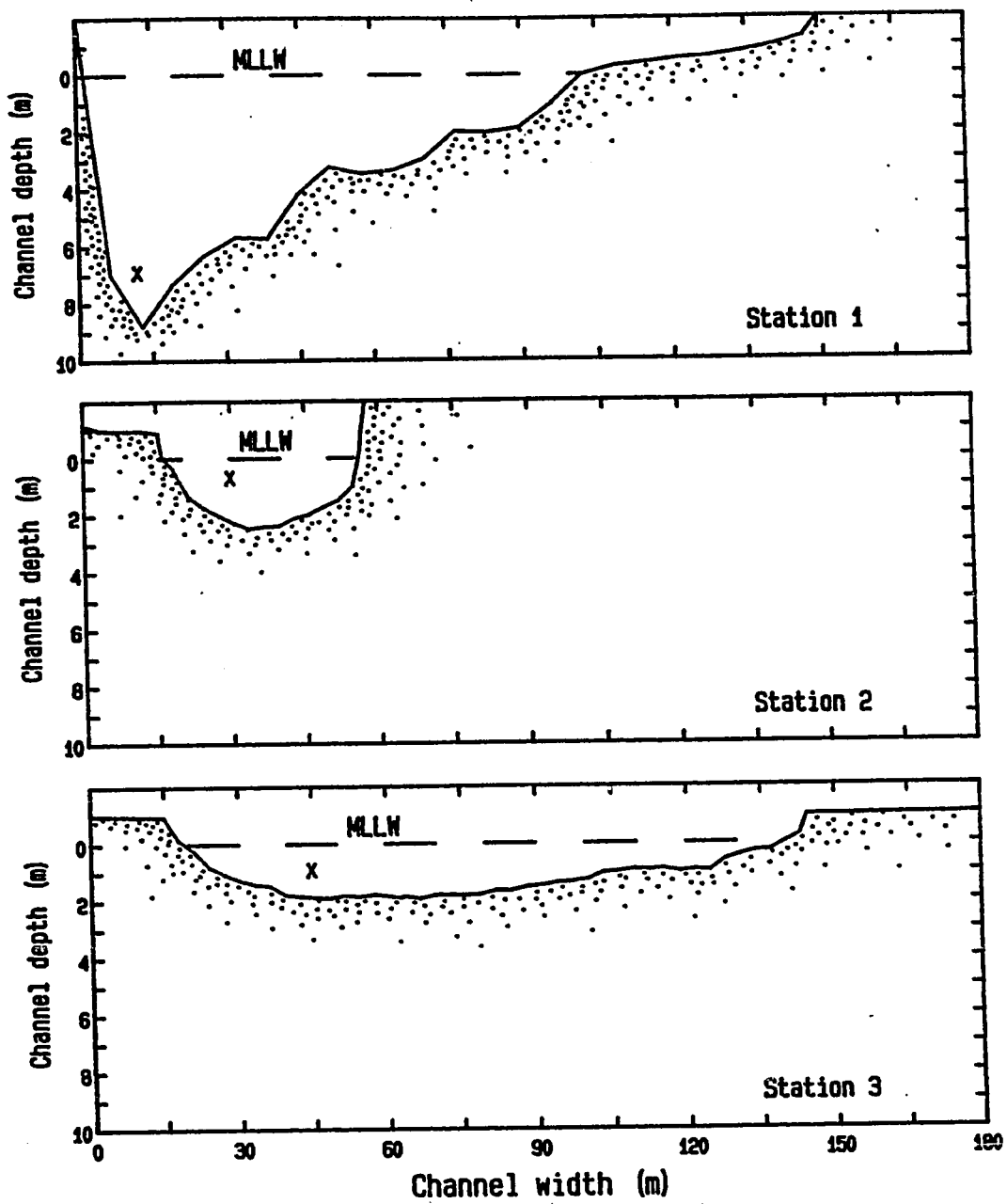


Figure 8. Cross channel profiles at stations where current velocity observations were taken. X shows the current meter location.

placed near each station, were surveyed to known National Ocean Survey (NOS) elevation bench marks. Surveying accuracy was ± 0.3 cm in vertical elevation over a 200 m distance. With the known water level elevation determined with pressure transducers, tidal heights was referenced to MLLW, the tide datum for the United States Pacific West Coast. The tide staff at station 1 was referenced to bench mark NOS 3623A 1976 with an estimated accuracy of ± 0.6 cm. Bench mark NOS 3623A 1976 was located on the north west corner of the old Highway 1 bridge abutment over Elkhorn Slough. Tide staffs at stations 2 through 4 were tied into bench marks NOS 3631A 1976 and NOS 3631B 1976. The estimated accuracy of the tide staff elevation was ± 0.3 cm at station 2 and ± 4.5 cm at stations 3 and 4, which were about 0.5 km away from the NOS bench marks. NOS bench marks NOS 3631A 1976 and NOS 3631B 1976 were located along the Southern Pacific (SP) Railroad right of way just north of the SP bridge that crosses the SM/PS channel.

A flat bottom slough boat was used to deploy, service, and retrieve the current meters. Current meters deployed at stations 1 through 3 were secured to bottom moorings constructed of 1.5 inch pipe and steel reinforcing bars (Fig. 9). Each corner was weighted by 20 lbs of lead for mooring stability. Endeco meters were bolted to swivels attached to the moorings, allowing for free horizontal rotation. S4 meters were bolted securely to the top of the

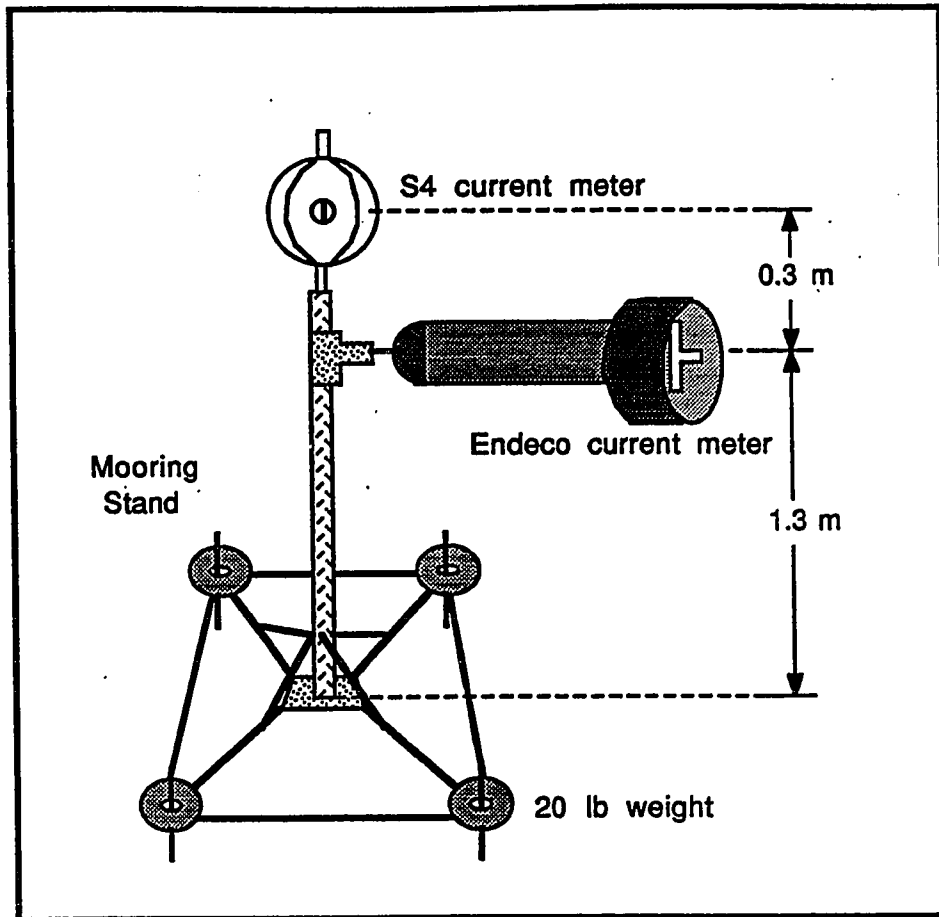


Figure 9. Current meter mooring configuration.

moorings.

At station 1, both Endeco meter # 100 and S4 meter # 04670917 were set in 7 to 9 m of water for current meter intercomparisons. At station 1, the Endeco meter was situated 1.3 m above the bottom and the S4 was secured 1.6 m above the bottom. At station 2, S4 meter # 0460916 was deployed 1.6 m above the bottom in 2 to 4 m of water. At station 3, Endeco meter # 101 was placed 1.0 m above the bottom in 3 to 5 m of water. This current meter was lowered from its initial deployment height of 1.3 m to 1.0 m when the mooring was nearly damaged by a fisherman's outboard motor. At station 4, Endeco meter # 102 was secured to a 3 m pole, 0.2 m above the bottom in 0.5 to 2.5 m of water. The purpose of this meter was to monitor only pressure (tidal height) and temperature.

The current meters were periodically serviced during slack tide to remove fouling by Enteromorpha sp. and kelp. Enteromorpha is a green algae commonly found growing along the tidal flats in Elkhorn Slough. During the warm summer months it is frequently found floating in thick mats throughout the middle and lower portions of Elkhorn Slough. Kelp grows subtidally in rocky portions of Monterey Bay and is occasionally washed into Elkhorn Slough on the flood tide. Kelp presented only an incidental concern in fouling the Endeco meter. Enteromorpha contributed the greatest problem in fouling the propeller of the Endeco meters. Of

the two Endeco meters recording tidal currents, virtually all the fouling occurred to the meter at station 1.

Tide staff readings were taken before and after each servicing to account for the depth change that occurred after each servicing period. The Endeco meter at station 4 was serviced only once to redeploy it into deeper water after it was apparent that its initial deployment was too shallow for tidal measurements during the lower low tides.

Data Processing

Hewlett Packard series 200 computers were used for data processing and analysis. Endeco current speed and direction were edited for current speed spikes. Spiking occurred at tide reversals before the meter could realign itself with the new direction of flow. Gaps in the data record during meter servicing periods were interpolated from data taken a half hour before and after each servicing period.

It will be shown later that flood and ebb flow do not simply reverse direction by 180° as would be expected by currents in long straight channels. Consequently, the average directions of flood and ebb flow were calculated separately to remove the "bend" in the channel axis between the reversing currents. First, current speed and direction were converted to their magnetic vector quantities to find the general axis of flood and ebb flow.

A vector approximating the flood axis was chosen and all flood current data that were within 30° of either side of this vector were assumed to be flood current. Observations outside the 30° bands were considered turbulent flow and were not included in calculating the directional flow along the channel axis. Velocities below 20 cm/s were also excluded because of noisy recorded current direction at low current speeds.

Using the above criteria the average flood direction was estimated. The original vector approximating the flood axis was replaced with the calculated flood axis and the process was repeated using a 15° band swath to either side of the calculated flood axis. The axis of flood current direction was determined by iteration until the average direction of flow was reproduced to 0.5° . This procedure was repeated for ebb currents and at each station. Following these corrections, Endeco current speed and direction data and S4 magnetic vector components were converted to their vector quantities aligned parallel and normal to the channel axis.

Pressure Correction

Preliminary analysis of pressure data indicated a variety of problems. The S4 pressure resolution, at station 1, was too coarse to be useful and pressure data from this meter were not used. The Endeco meters at

stations 1 and 4 appeared to have a temperature effect and pressure data at station 1 appeared to be attenuated by 30% based upon comparisons to Monterey predicted tides.

Correction of the temperature effect required taking pressure readings at constant pressure but varying temperature. These data were obtained by varying temperature at atmospheric pressure before field deployment. The algorithms for temperature correction for the Kavlico pressure transducers were:

$$P_{100} = X + 5.0 * (293.5 - T)$$

$$P_{102} = X + 2.4 * (293.5 - T)$$

where P is temperature corrected pressure, X is uncorrected pressure, 293.5 is the reference temperature in °K (recorded temperature of current meter when assembled for deployment), T is observed temperature in °K, and the constants 5.0 and 2.4 are pressure correction coefficients.

Fluctuations in back pressure on the pressure transducer resulting from temperature changes in an enclosed meter housing caused the observed pressure variations. The pressure calibrations were made with the sensors and electronics outside of the meter housing at atmospheric pressure. The reference temperature for the pressure correction was, therefore, taken as the recorded temperature of the current meter at the time that the current meters were assembled prior to deployment. No

discernible temperature effect was noted for meter # 101. Correlations of tidal height between the pressure transducers and tide staff observations, at each station, indicated that observed tidal heights are corrected to within ± 0.1 m of MLLW (Fig. 10).

Comparison of Endeco and S4 current meters

One Endeco and an S4 meter were deployed simultaneously at station 1, during the September time series. Concurrent 30 min vector averaged velocity and temperature data were compared between the meter types. Current velocities measured by the Endeco and S4 meters were in good agreement as long as the Endeco remained free of fouling (Fig. 11A). Velocity measurements recorded immediately after servicing were essentially equivalent for both meters. As entangling green algae retarded impeller motion, observed current velocities decreased for the Endeco meter (Figs. 11B and 11C). S4 current observations were as much as 40% higher than Endeco measured currents at peak current flow during periods of fouling (Fig. 11B). The magnitude of fouling is similar to that found in a field study comparing Endeco and S4 current meters in San Francisco Bay, where the S4 meter was found to indicate speeds 20 to 50% higher than the Endeco meter during periods of maximum ebb and flood flow (Gartner and Oltuman, 1985).

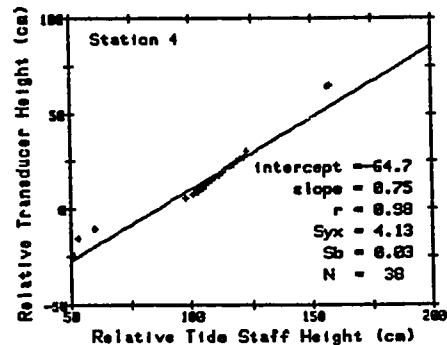
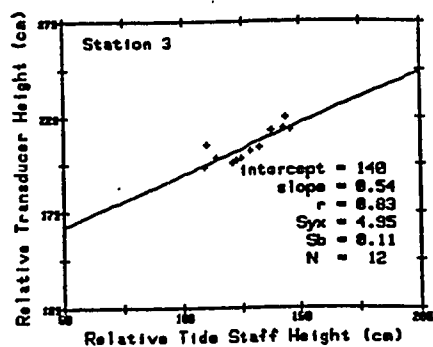
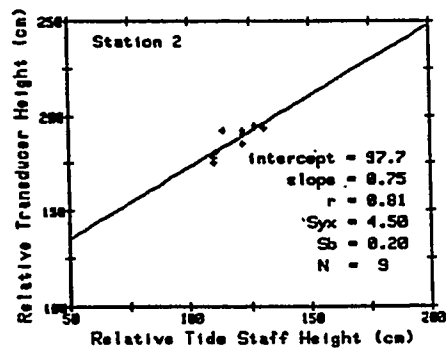
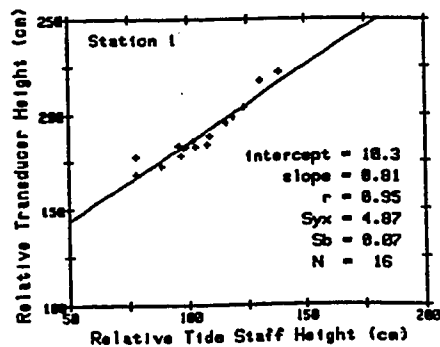


Figure 10. Correlation between uncorrected pressure transducer tidal height with uncorrected tide staff tidal height.

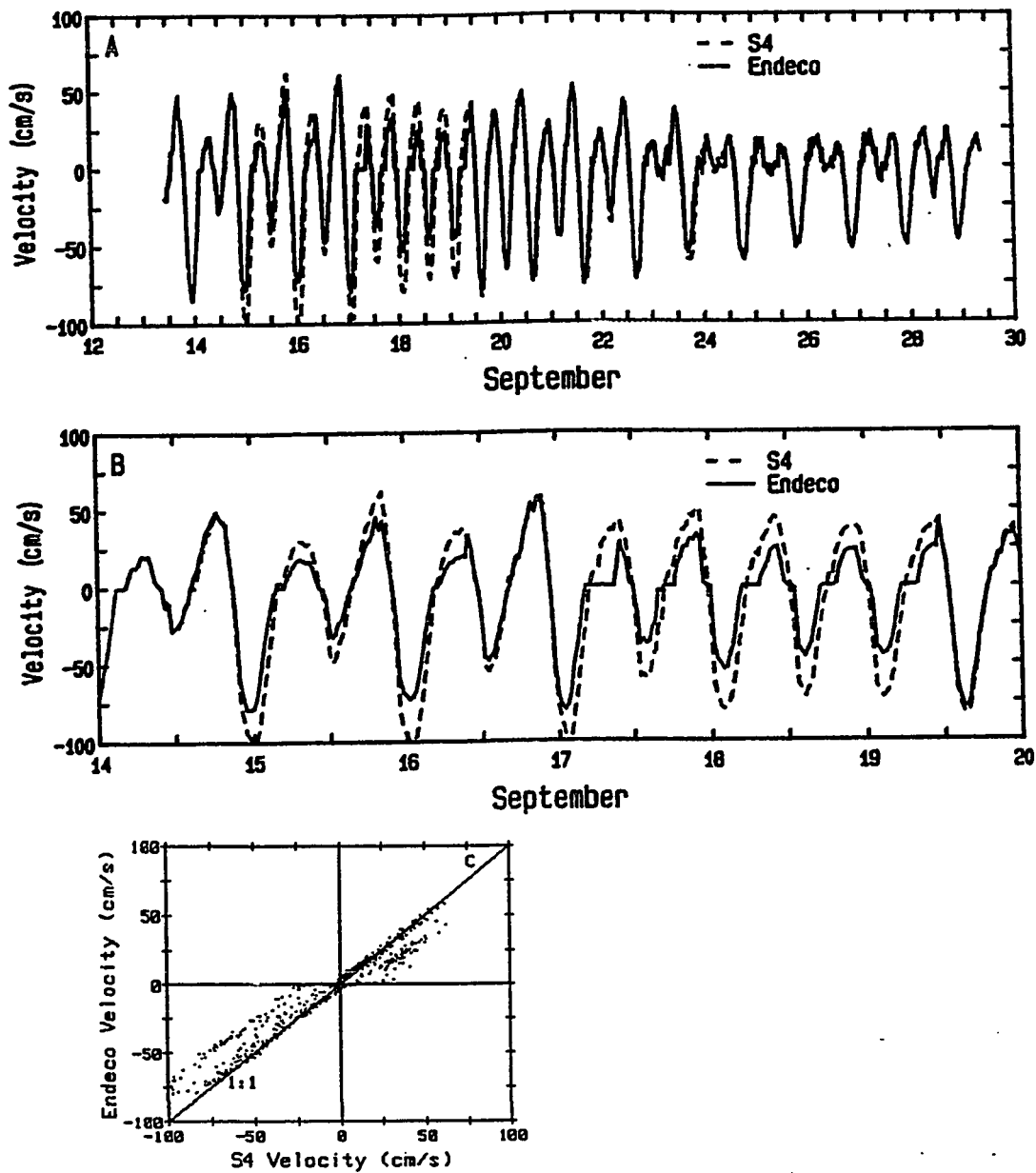


Figure 11. A) Comparison of Endeco and S4 current velocities at station 1. B) Closeup showing a major Endeco fouling period. C) Correlation between Endeco and S4 current velocities.

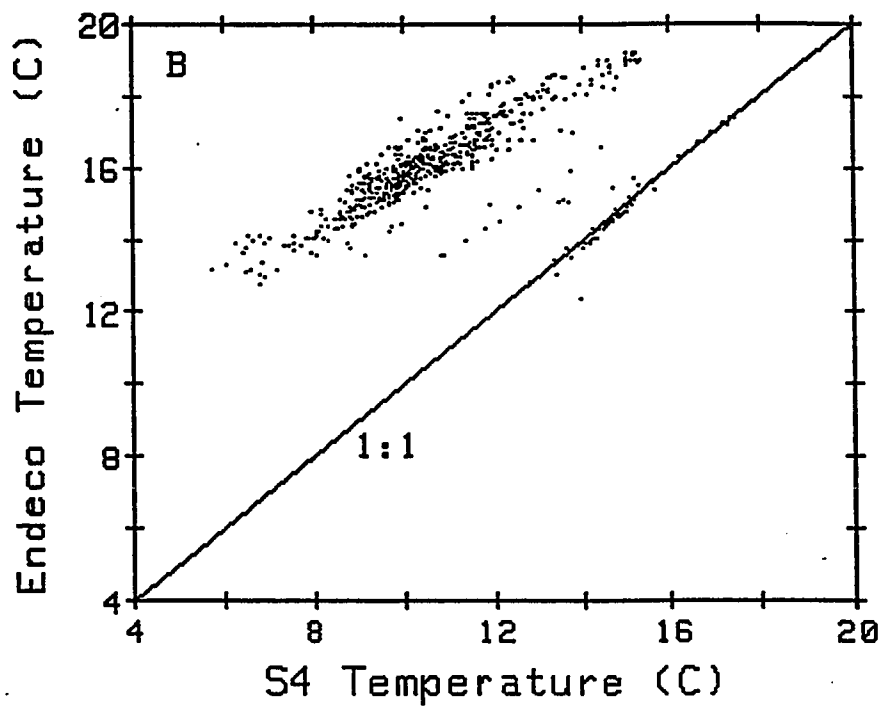
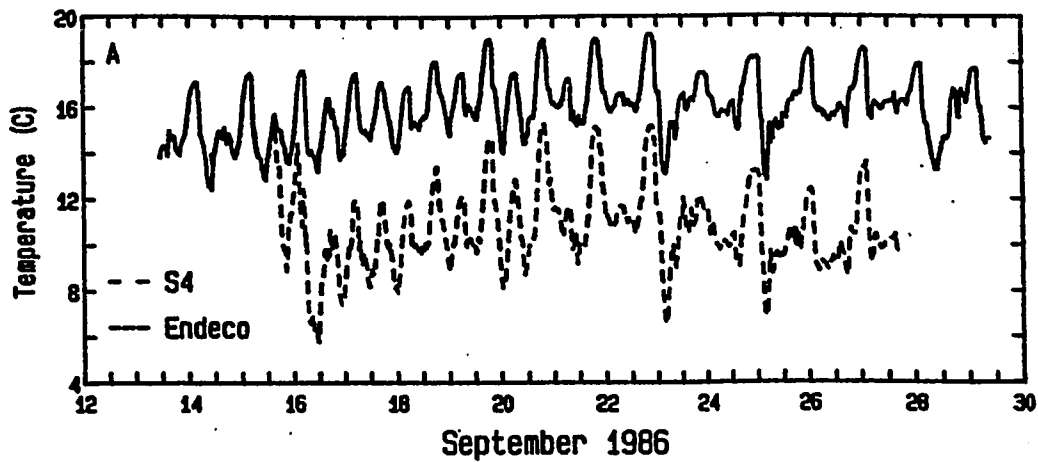


Figure 12. A) Comparison of water temperature between Endeco and S4 meters at station 1. B) Correlation between Endeco and S4 temperature. Note temperature offset in the S4 meter begins on 15 September 1986.

Endeco and S4 directional data agreed well. Initially, temperature measurements were well correlated. However, approximately two days into the S4 deployment, 15 September, an electronic problem caused periodic offsets in the temperature data (Fig. 12). Pressure measurements were not directly comparable between the two meters because of low resolution of the 1000 m range pressure transducer in the S4 current meter.

Comparison of Endeco and S4 current velocity measurements indicate a good correlation between the meter types when the Endeco was not fouled. Since the Endeco meter was prone to fouling, only the S4 current observations were used for this station. Conversely, temperature and tidal height data were taken only from the Endeco meter at station 1.

Vertical Profile

A profile of the vertical velocity distribution was conducted to resolve current observations in the benthic boundary layer to sectional mean velocity. Velocity profile measurements were taken only at station 1, where the meters were moored within the boundary layer. Velocity measurements at stations 2 and 3 were assumed to be outside the boundary layer because they were deployed at mid-channel depth, so no profiles were taken at these stations.

Vertical velocity profiles were observed using an S4 current meter and a NEC laptop computer to obtain real time data. Current observations were sampled at 1 m intervals between the surface and the bottom, and vector averaged at 0.5 sec intervals for 1 min. Velocities were observed at peak flood and ebb flow to obtain observations as close to a steady flow condition as possible, and the averaging interval was kept short to minimize trends in velocity changes over time. All current velocity observations, at station 1, have been corrected to nonboundary layer velocities and are reported as such in this report.

RESULTS and DISCUSSION

Tidal Elevation

Changes in tidal elevation were measured to compare tidal ranges in the slough to Monterey predicted ranges. The times of highest and lowest water were used to determine rise and fall duration and phasing of the tide. The duration of rising and falling water can be an important parameter in influencing the strength of flood and ebb tidal currents (see below). Observed phase lags of high and low water were compared to predicted lags, derived from tidal constituents estimated before slough restoration, to determine changes in tidal phase lags.

The mixed semidiurnal tide characteristic of Elkhorn Slough is the major feature shown in the tidal record (Fig. 13). The tidal record indicated unequal tides that began during the spring tide with a diurnal range of about 2 m. The time series continued through the neap cycle and reentered the spring tide before the observations were completed. Spectral analysis of 30 min averaged data confirmed that the majority of the tidal height variance was concentrated in the semidiurnal (0.081 hr^{-1}) and diurnal (0.040 hr^{-1}) periods accounting for 98% of the total variance at all four stations (Fig. 14).

The greatest tidal height variation came from the semidiurnal period followed by the diurnal period. The

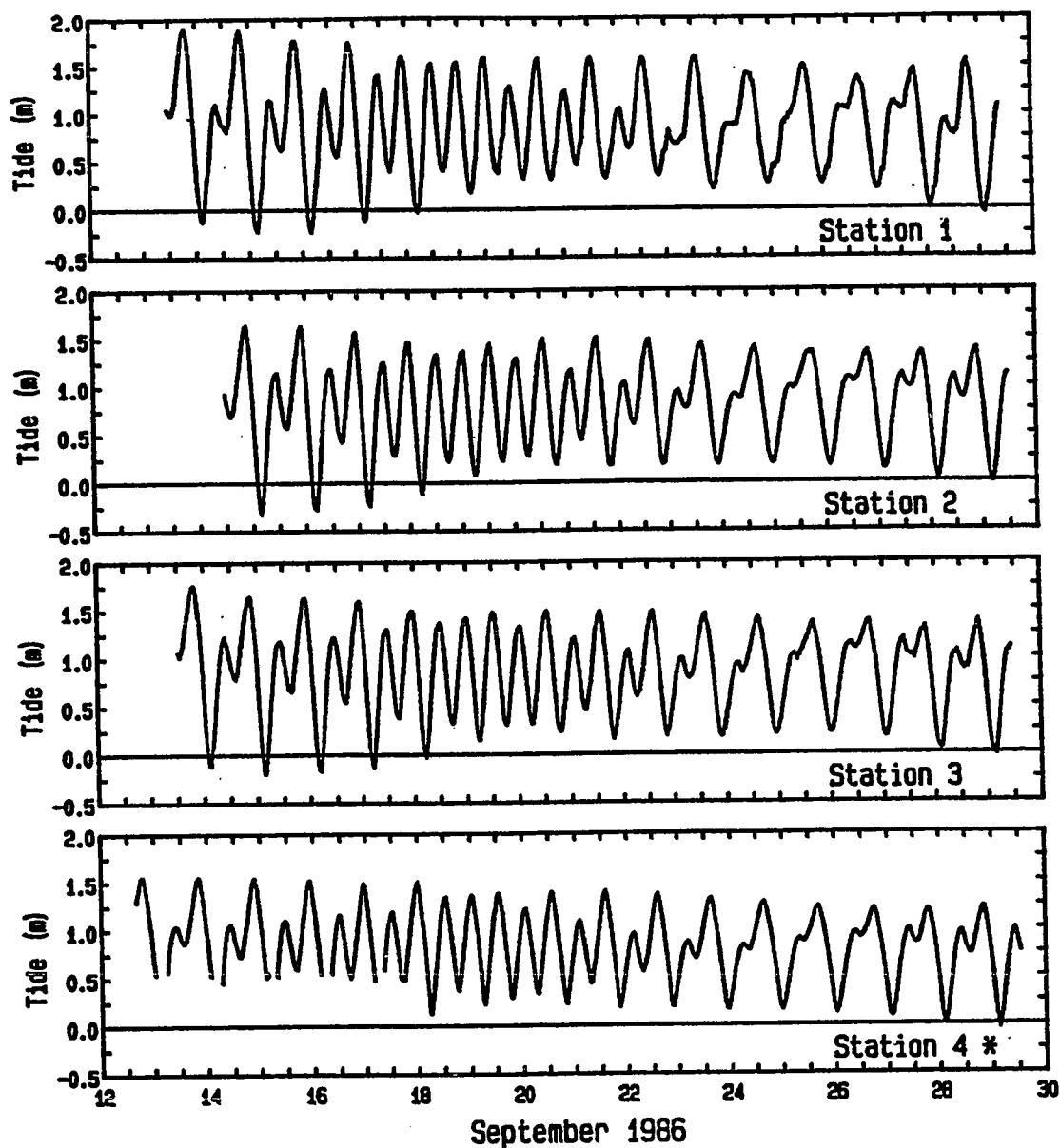


Figure 13. Time series of corrected observed tides at stations shown in Fig. 7.
 * Gaps in tidal record indicate missing data during shallow meter deployment at station 4.

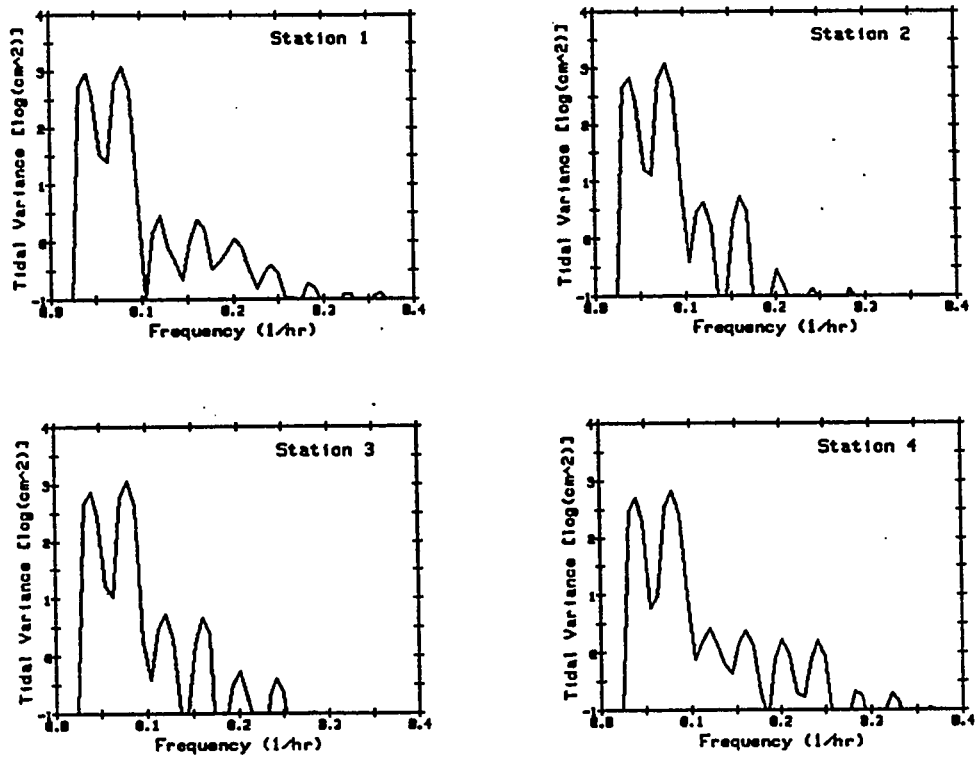


Figure 14. Tidal height spectra at stations in Fig. 7.

next two largest spectral peaks were centered in the 0.121 hr⁻¹ (8.3 hr) and 0.161 hr⁻¹ (6.2 hr) frequencies and account for 0.2 to 0.3% of the remaining tidal variance (Fig. 14 and Table 3). The magnitude of the 8.3 and 6.2 hr variances doubled from 0.1% at the slough's entrance to 0.2 to 0.3% of the total variance at the inland stations, while the magnitude of the semidiurnal variance decreased in the inland direction (Table 3).

Table 3. Variances of tidal elevation of the four largest tidal periods, derived from spectral analysis.

Period (hr)	Station							
	1		2		3		4	
	(cm ²)	(%)	(cm ²)	(%)	(cm ²)	(%)	(cm ²)	(%)
24.8	1940	44.9	1400	38.2	1460	40.0	987	42.8
12.4	2310	53.5	2210	60.2	2140	58.9	1270	55.1
8.3	4.9	0.1	7.8	0.2	10.5	0.3	5.6	0.3
6.2	4.9	0.1	10.4	0.3	8.8	0.2	5.2	0.2

Percent variation is of the total variance.

The 8.3 hr, teridiurnal and 6.2 hr, quarterdiurnal periods are shallow water constituents. The teridiurnal compound constituents (MK₃ and 2MK₃) are the result of the sum and the difference of the speed numbers of the principal constituents (M₂ and K₁). The quarterdiurnal harmonic (M₄) is an overtide of the M₂ constituent, its speed number is exactly double that of the M₂. These shallow water constituents are an important characteristic of tides in the slough and will be discussed below.

The observed tidal ranges at stations 2, 3 and 4 were 97, 94 and 87% of Monterey predicted tides. However, the uncorrected range at station 1 (not shown) was only 69 % of Monterey predicted tides. The tidal ranges at stations 1 and 4 were independently compared to Monterey predicted tides by tide staff observations during a spring tide in August 1988 (Fig. 15). Relative tide elevations were observed at 0.5 hr intervals for 27 hrs at each station. These tide staff observations indicated that the tidal ranges at stations 1 and 4 were 99 and 94% of Monterey predicted tides, and suggest errors in the pressure transducer measurements.

The partial collapse of the oil filled septum that encased the sensing element of the Endeco pressure transducer used at station 1 is probably responsible for the attenuated tidal range observed at this station. Tidal heights at station 1 were corrected to Monterey predicted ranges because station 1 is located near the bay (and should respond like Monterey tides), the other observed tidal ranges were larger, and the observed tide staff ranges, at station 1, were within 99% of Monterey ranges (Fig. 15A). Therefore, all consequent analyses were made with the corrected data (Fig. 13A). At station 4, a 7% difference between the transducer range (87% of predicted) and tide staff range (94% of predicted) was observed. However, no physical aberrations of the pressure

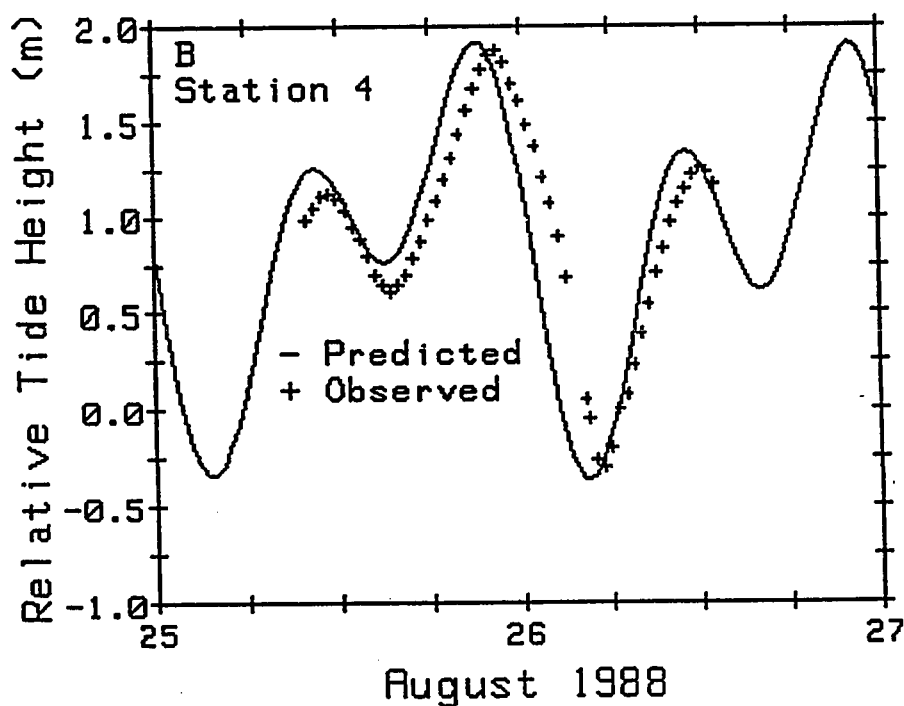
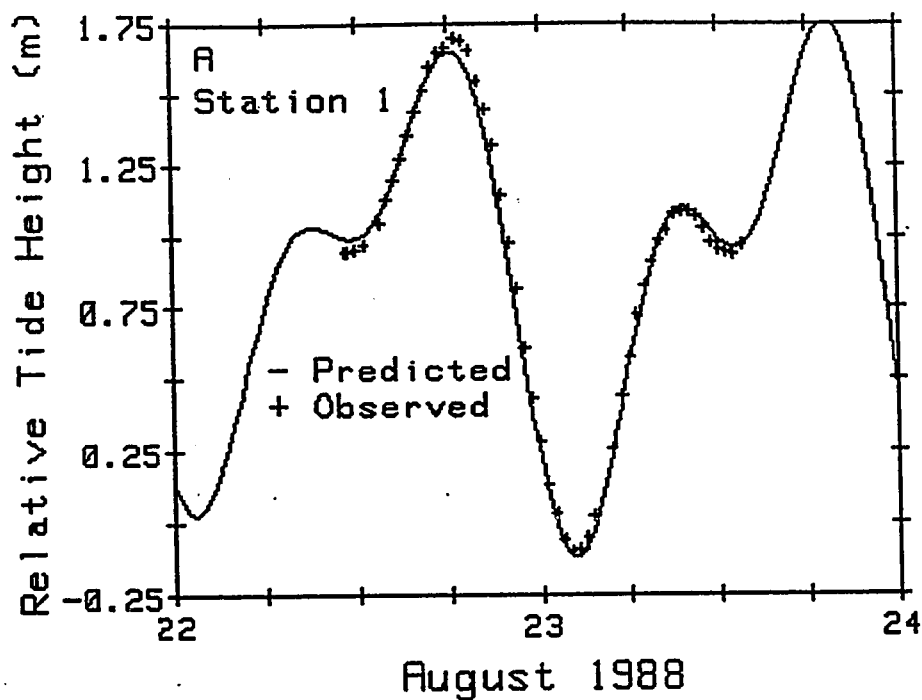


Figure 15. Comparison of relative tide staff heights with Monterey predicted tides (based on NOAA constituents).
A) slough entrance B) South Marsh.

transducer assembly were noted to justify editing the attenuated pressure signal.

The 7% increase (relative to predicted tides) in transducer tidal ranges, from September 1986, to the tide staff ranges, in August 1988, may be due to erosion of the dike that restricted water flow into the South Marsh. Strong tidal currents may have eroded the dike between 1986 and 1988, allowing greater volume transport into the South Marsh and increased the tidal range.

Slough restoration has had little effect on the tidal range of the main channel of the slough. The observed ranges at station 2 were 3% less than Monterey predicted ranges, based on tidal constituent estimates. This range is the same as the mean predicted range at NOAA's station # 493, which is also 3% less than Monterey predicted tides (NOAA tide tables, 1986).

Table 4. Mean duration of rising and falling water.

Period	Station			
	<u>1</u> Time (hr)	<u>2</u> Time (hr)	<u>3</u> Time (hr)	<u>4 *</u> Time (hr)
Combined	6.2	6.2	6.2	6.2
Rise	6.4	7.1	7.0	6.9
Fall	6.0	5.4	5.5	5.6
Asymmetry	0.4	1.7	1.5	1.3
* Mean duration calculated from tide data after shallow meter deployment at station 4.				

Duration of Rising and Falling Water Level. The duration of rising and falling water in Elkhorn Slough is dependent on friction in a shallow channel, the inefficient transport of water over tidal flats and the unequal range of the mixed tides (Fig. 4). Friction in a shallow channel decreases rising water duration, while tidal flats and unequal tides common to Elkhorn Slough increase rising water duration. The implication of a longer or shorter duration of rising or falling water is that tidal currents are higher in either the flood or ebb direction. This usually leads to either deposition or erosion of sediment into or out of the system.

The duration of rising and falling water was analyzed to document the magnitude of tide asymmetry in the slough. A five point binomial filter was used to smooth the two-minute tidal height data to remove spurious high frequency tidal elevation noise from the level of high and low water. These filtered data were used to determine the times of high and low water level. The average duration of the observed half-tide cycle was 6.2 hr. However, the duration of rising water is longer than falling water (Fig. 16 and Table 4). The shortest mean duration of rise was 6.4 hr, at station 1, and the longest was 7.1 hr, at station 2. The longest mean duration of fall was 6.0 hr, at station 1, and the shortest was 5.4 hr, at station 2. Stations 3 and 4 were similar to station 2 with

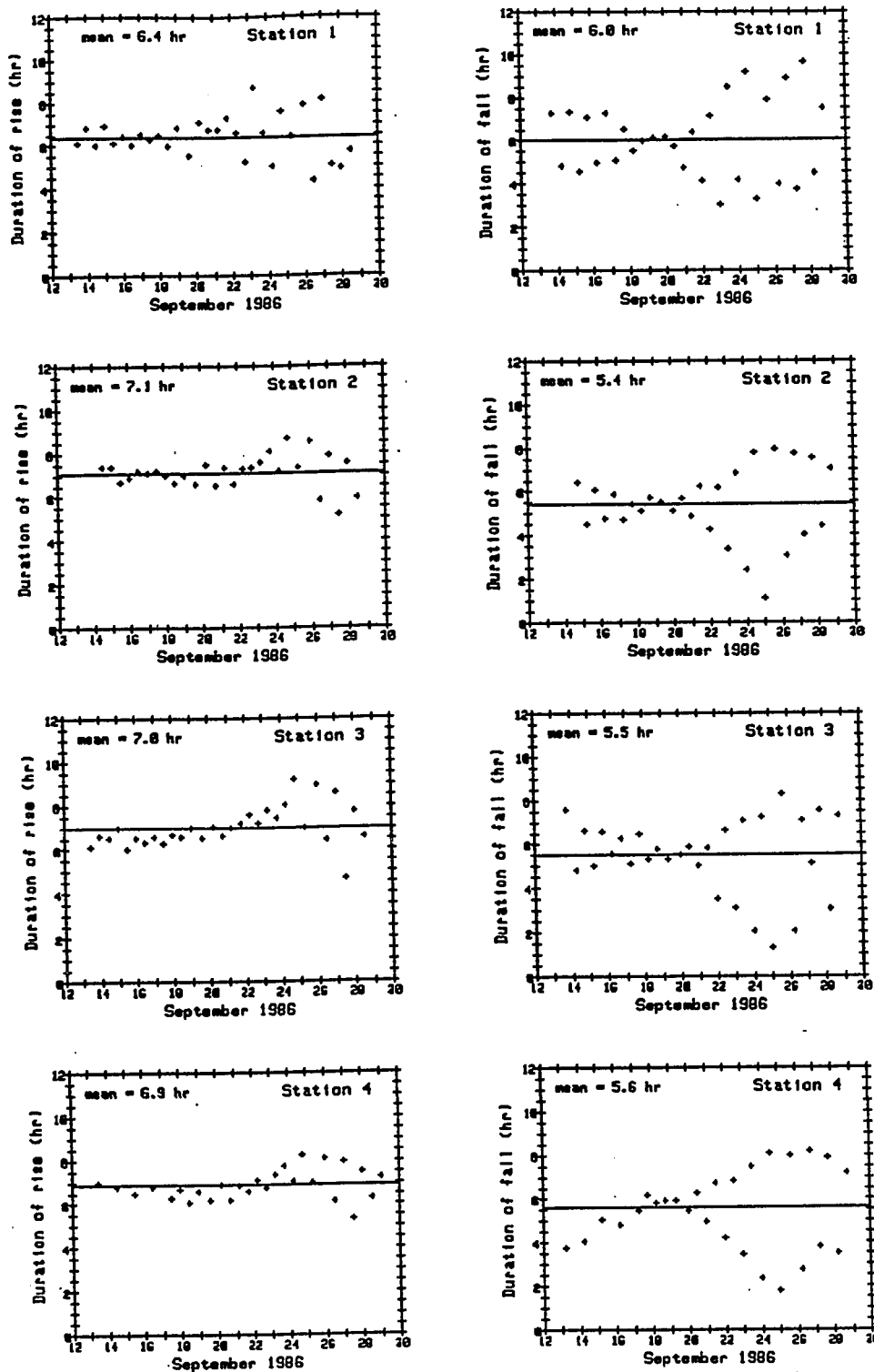


Figure 16. Duration of rising and falling water at stations shown in Fig. 7. Horizontal line shows mean duration listed on graph.

substantially longer rising tides than falling tides (Fig. 16 and Table 4). Note, although the mean durations of rising and falling water are not significant in a statistical sense, there is still meaning in the values in a physical sense.

Elkhorn Slough exhibited a tidal asymmetry that is characteristic of "ebb dominant" systems. Ebb dominance has been attributed to the inefficient water exchange between tidal flats and tidal channels at high water (Speer and Aubrey, 1985; Friedrichs and Aubrey, 1988). In tidal embayments where the ratio of intertidal volume is large relative to channel volume, friction over intertidal marshes and flats can cause high tide to propagate slower than low tide. In effect, tidal flats store water without transporting momentum. The inefficient transport of water over tidal flats causes high tide to lag longer than low tide, resulting in short duration ebb tides (Speer and Aubrey, 1985; Friedrichs and Aubrey, 1988). Time asymmetry is a cumulative effect and increases as the tidal crest progresses up an embayment.

Ebb dominance, which is characterized by short durations of falling water and higher ebbing tidal currents, is an attribute of Elkhorn Slough which can be illustrated by the difference in the duration of rising and falling water at each station (Fig. 16). Station 1, located near the slough entrance, exhibited the least amount of

time distortion from a sinusoidal ocean tide. As the tidal crest progressed up the slough, tidal flat area and time asymmetry between rising and falling water increased. Station 2, located in a channel that communicates with an area having a large tidal flat to channel ratio (Fig. 7), showed the longest time asymmetry of 1.7 hr. Station 3, located in the main channel approximately mid-way up the slough, indicated a difference of 1.5 hr (Table 4).

Station 4, located at the head of the South Marsh in the Research Reserve, displayed only a 1.3 hr difference between rise and fall durations. It might be expected that this difference should be longer since the South Marsh is located in an extensive tidal flat area and is isolated by a shallow narrow channel. However, the small tide asymmetry observed may be explained by Aubrey and Speer's (1985) observation that time asymmetry can virtually disappear during neap tide. At station 4, spring tide durations were not observed because the pressure sensor was above water at lowest low tide (Fig. 13). Thus, the mean durations of rising and falling water were biased by a lack of observations during the spring tides, perhaps accounting for a smaller tide asymmetry.

Tide asymmetry can be represented as a phase difference between significant shallow water constituents relative to their predominant astronomical constituents. Figure 17 illustrates the tide asymmetry produced by the M_2

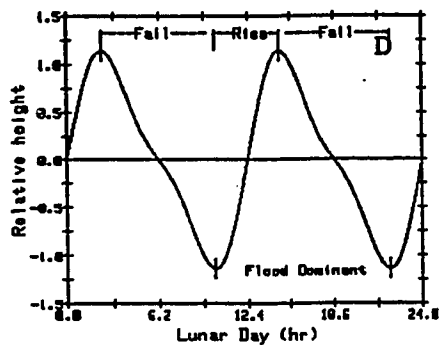
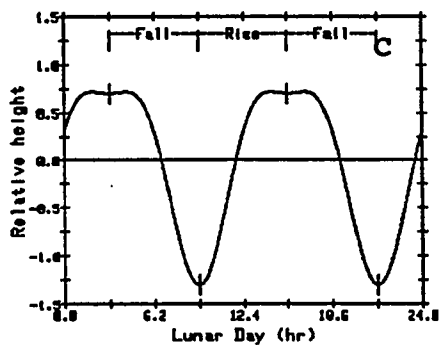
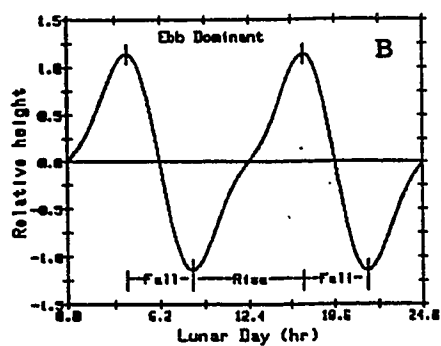
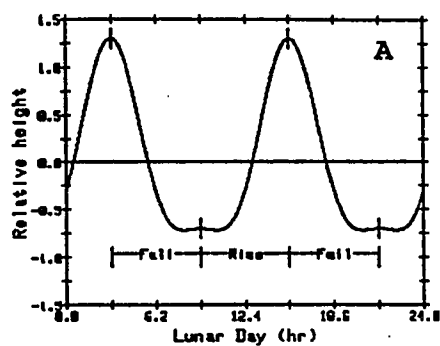


Figure 17. Model of tide asymmetry produced by different phasing of M_2 and M_4 constituents. M_4/M_2 amplitude ratio = 0.3. A) phase = 0° B) phase = 90° C) phase = 180° D) phase = 270°

and its overtide, M_4 , at different phasing. When phase differences between M_2 and M_4 are 0° or 180° a symmetric tide is produced. At 0° phase difference, M_2 and M_4 sum to produce extreme high tides but interfere at low tide to produce moderate low tides (Fig. 17A). The reverse occurs when the phase difference is 180° , producing extreme low tides and moderate high tides (Fig. 17C).

Nonsymmetric tides are generated when the shallow water constituent, M_4 , leads or lags the M_2 constituent; the maximum effect occurs when the phase difference is 90° . When M_4 leads M_2 , duration of falling water is longer than rising water, resulting in a "flood dominant" tide (Fig. 17D). When M_4 lags M_2 , duration of falling water is shorter than rising water, resulting in an "ebb dominant" tide (Fig. 17B).

Tidal wave asymmetry has been modelled using only the M_2 and M_4 constituents, along the east coast of the United States. Since the east coast tide is typically classified as semidiurnal, the K_1 constituent does not play a major role in producing tides. However, along the U.S. west coast, including Elkhorn Slough, the tide is classified as mixed, mainly semidiurnal. Both the M_2 and K_1 constituents play a major role in tide generation here.

Tide asymmetry can be represented by comparing the duration of rising and falling water of the primary astronomical constituents with the duration of rising and

Table 5. The primary astronomical and shallow water constituents used to model tide duration asymmetry in Elkhorn Slough, based on NOAA station # 493 tide constituents.

Constituent	Speed # (deg/hr)	Height (cm)	kappa (deg)	kappa (hr)
K ₁	15.041069	35.60	103.0	6.8
M ₂	28.984104	49.68	303.7	10.5
M ₄	57.968208	1.34	356.5	6.1
Mk ₃	44.025173	1.52	185.4	4.2
2MK ₃	42.927140	1.34	196.2	4.6

falling water of the sum of the primary and major shallow water constituents. This process was used to model tide asymmetry in Elkhorn Slough (Table 5). The constituents used for this analysis were taken from NOAA constituents obtained during a 365 day time series in 1976, at station # 493, called Elkhorn, Elkhorn Slough (Appendix 2). This station is situated less than 0.5 km inland from station 3. Tide predictions generated from these constituents were used to observe the impact of shallow water constituents on tide asymmetry relative to the primary semidiurnal and diurnal constituents (Fig. 18). Predictions using only K₁ and M₂ produced mean durations for both rising and falling water of 6.2 hr (Figs. 18A and 18B). However, tidal durations of the larger semidiurnal tidal ranges were always greater than 6.2 hr, while durations of the smaller ranges were less than 6.2 hr. Predictions which included the shallow water constituents M₄, MK₃ and 2MK₃, as well as K₁ and M₂,

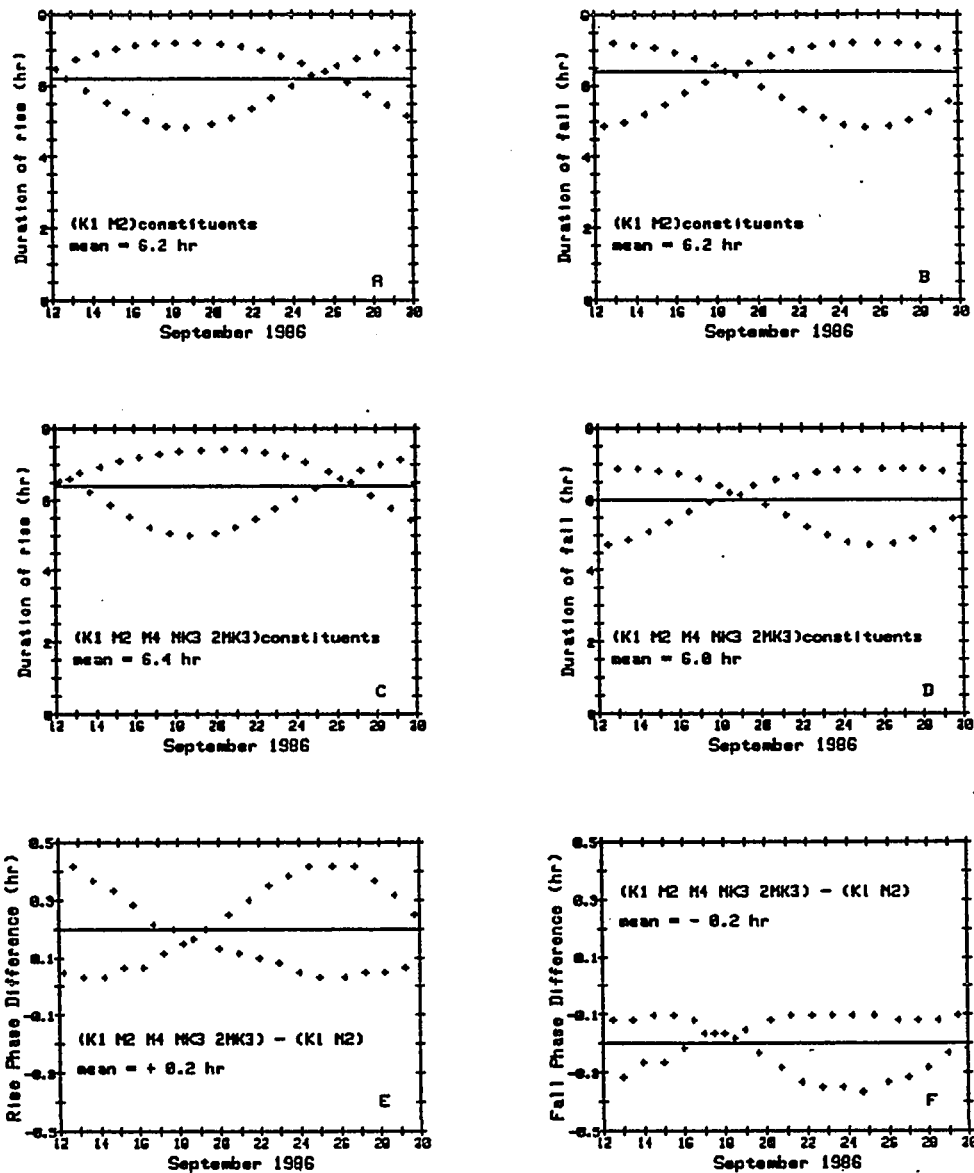


Figure 18. Duration and the difference in duration of the predicted tides using the (K₁ M₂) and (K₁ M₂ M₄ MK₃ 2MK₃) tidal constituents (based on 1976 NOAA station # 493 tide constituents). Horizontal line shows mean duration listed on the graph.

followed the same pattern of longer durations for larger tide ranges and shorter duration for smaller ranges (Figs. 18C and 18D). In addition, these predictions resulted in a longer mean rise duration of 0.2 hr and a shorter mean fall duration of 0.2 hr, over the K_1 and M_2 predictions (Figs. 18E and 18F). The tide asymmetry represented in the production of shallow water constituents suggests that this technique may be useful in determining tide asymmetry of tidally influenced systems along the Pacific West Coast.

Slough restoration has increased the ratio of tidal flat to channel volume, causing an increase in tide asymmetry in the ebb dominant direction. Tide predictions at station # 493, using 1976 constituents (Table 5), for September 1986, showed that the duration of rise would be an average of 0.4 hr longer than the fall (Fig. 18E and 18F). However, the observed tides, during September 1986, at station 3, indicated that the duration of rise lasted 1.5 hr longer than fall. The increased asymmetry in tide duration was likely the result of an expanded water storage capacity over the tidal flats which retarded the propagation of high tide. Additional salt marsh restoration in the slough will probably enhance ebb dominance further.

Phase Lags. Local phase lag of high and low water has doubled since 1976. The mean tidal lags at each station,

Table 6. Phase lag of high and low water relative to Monterey predicted tides, during September 1986.

Station	High (hr)	std. dev. (hr)	Low (hr)	std. dev. (hr)
1	-0.1	0.5	-0.1	0.7
2	0.8	0.4	0.2	0.3
3	0.7	0.3	0.2	0.2
4 *	0.8	0.4	0.8	0.3
493 +	0.3		0.1	
+ Station # 493 from NOAA tide tables.				
* Lag time of extreme tide ranges not obtained from 12 to 17 September, at station 4.				

relative to Monterey predicted tides, were calculated from two-minute filtered tidal height data (Table 6). Time of high and low water at the slough entrance (station 1) generally occurred 0.1 hr earlier than Monterey predicted tides and lagged later as the tidal crest progressed inland. A comparison of mean lag times indicated that the lag had apparently doubled at station 3, relative to station # 493, since tidal constituents were estimated in 1976 (Appendix 2). This gives further evidence of the impact that the restored areas have had on the tidal characteristic of Elkhorn Slough.

Temperature

Although an analysis of temperature in Elkhorn Slough was not a primary objective of this study, the temperature data showed some interesting features. The mean water

Table 7. Observed water temperature during September 1986.

Statistic	Station			
	1	2	3	4
mean	15.9	17.7	17.9	18.4
std. dev.	1.4	1.2	1.3	1.1
minimum	12.3	14.6	14.5	15.7
maximum	19.2	21.1	20.6	22.0

temperature in September 1986, at station 1, was 15.9°C and increased in an inland direction to 18.4°C, at station 4 (Table 7). The lowest recorded temperature was 12.4°C, at station 1, and is representative of September surface temperature of central Monterey Bay water (Dr. William Broenkow, per. comm.). Solar insolation increased slough water temperatures to a maximum of 22.0°C, at station 4.

The temperature structure during the time series appeared to be typical for Elkhorn Slough during September (Smith, 1974; Nybakken *et al.*, 1977). The average temperature increased in an inland direction by approximately 2°C along the main channel.

A semidiurnal temperature fluctuation (Fig. 19) was inversely correlated with the semidiurnal period of tidal height, at stations 1 through 3. Spectral analysis confirmed that the temperature variance was concentrated in the semidiurnal (0.081 hr^{-1}) and diurnal (0.040 hr^{-1}) periods (Fig. 20), and water temperature was about 180° out of phase with tidal height (Table 8).

In terms of tidal flux, the inverse relation between

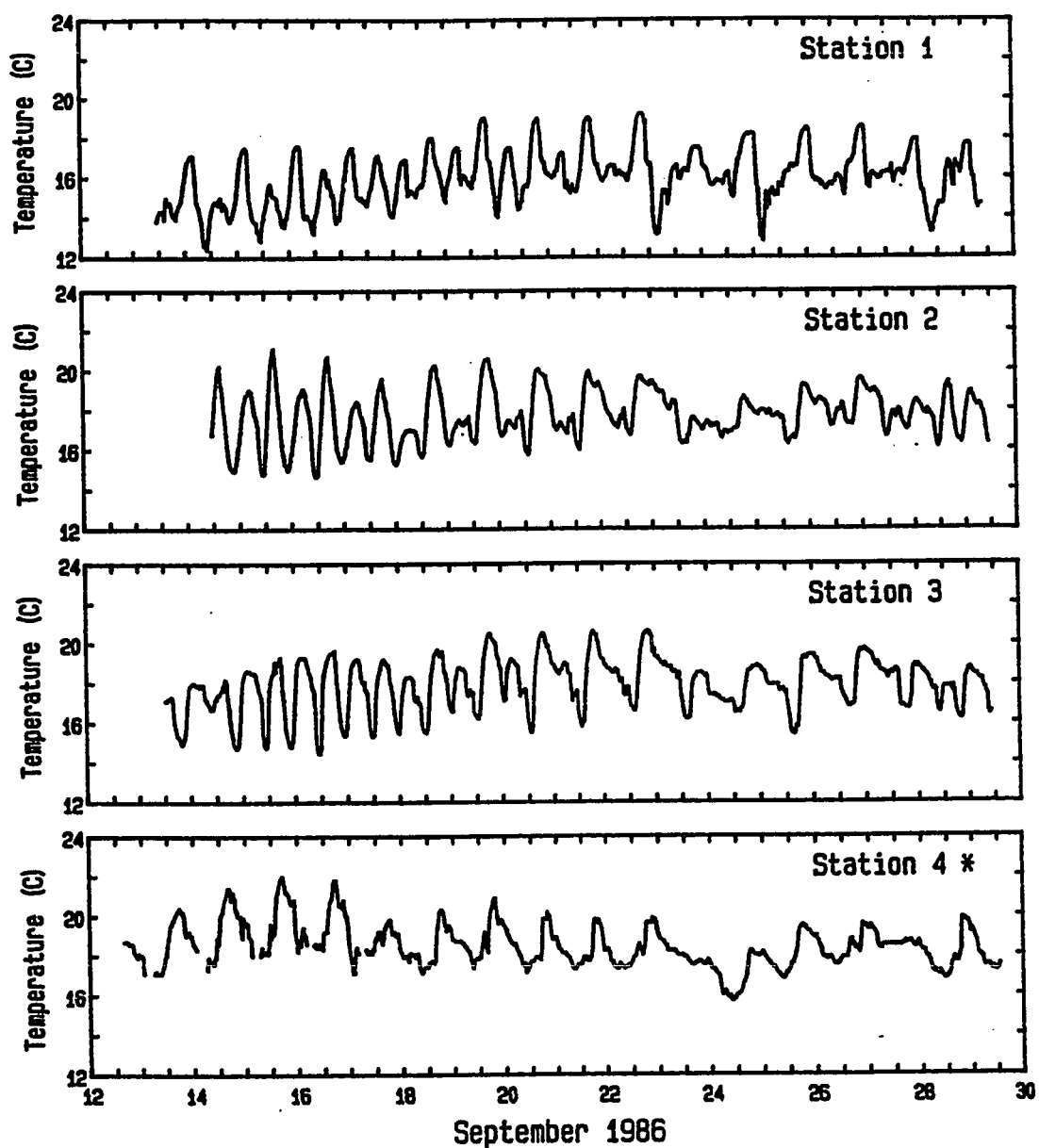


Figure 19. Time series of observed water temperature at stations shown in Fig. 7.
* Gaps in temperature record indicate missing data during shallow meter deployment at station 4.

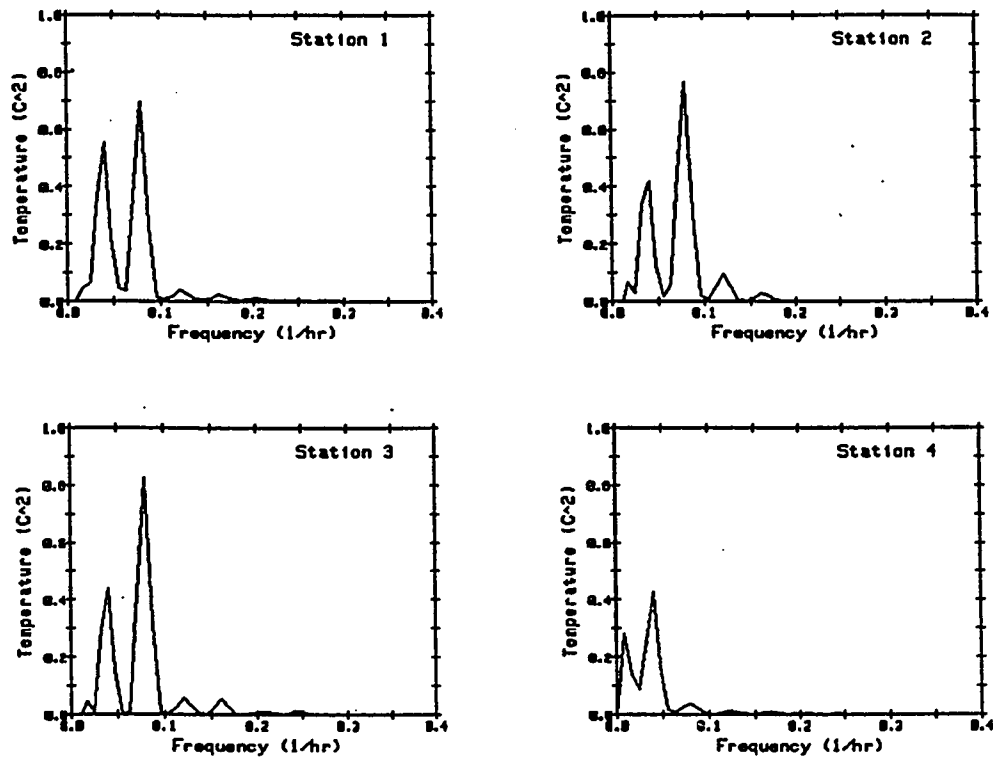


Figure 20. Water temperature spectra showing large diurnal and semidiurnal variances at stations 1 through 3, but only large diurnal variance at station 4.

Table 8. Phase lag and variance between the time of highest tide height and the time of highest water temperature for the semidiurnal period, derived from cross spectral analysis.

Station	Phase (deg)	Co-variance (deg*cm)
1	190	1225
2	193	1165
3	177	1134
4	165	663

temperature and tidal height was associated with advection of warm upper slough water flushing out into Monterey Bay on the ebb tide, and cold Monterey Bay water returning to Elkhorn Slough on the flood tide. A significant temperature variation between high and low tide is one indication that much of the water expelled from the slough on the ebb tide does not reenter Elkhorn Slough on the flood tide. This result agrees with conclusions observed by Smith (1974) and Reilly (1978) that the majority of water leaving the slough on the ebb tide does not return to Elkhorn Slough.

In contrast to the stations located in tidal channels, station 4 exhibited a predominantly diurnal (0.040 hr^{-1}) periodicity (Fig. 20D). Temperatures peaked during early evening and dropped to a minimum during early morning. This periodicity follows the typical pattern of the daily heating cycle of surface water in an enclosed body of water (Knauss, 1978). Since station 4 is located at the head of

the South Marsh, water from other segments of the slough does not flow through this site. Thus, water temperature here is not as strongly influenced by tides as are the channel areas.

Temperature, in the South Marsh, is affected more by solar radiation and sensible heat exchange with the atmosphere than advection of water from other parts of the slough. A least squares regression of daily mean temperature with daily mean solar irradiance (MLML weather report, unpublished) initially showed a poor correlation ($r = 0.27$)(Fig. 21A). However, when solar irradiance values were lagged by a day, the correlation value doubled ($r = 0.58$)(Fig. 21B). The lagging effect is the result of weighting the daily mean values to noon of each day. Because highest water temperature is attained during the evening, this has the effect of lagging observed water temperature by a day relative to the irradiance observations. When the lag effect was removed, 34% (r^2) of the change in water temperature was explained by the change in daily solar irradiance.

When solar insolation is converted to thermal heating of slough water, a correlation between solar insolation and mean water temperature can be made, such that:

$$T = E_{\text{total}} / Z_{\text{mean}} * C_p / d,$$

where T is potential thermal warming of the slough water,

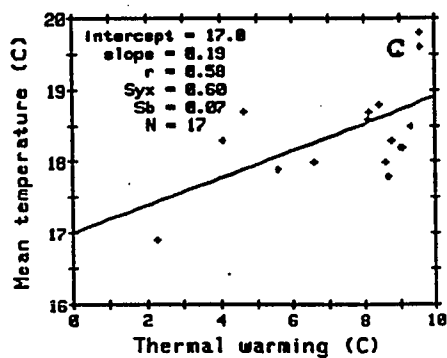
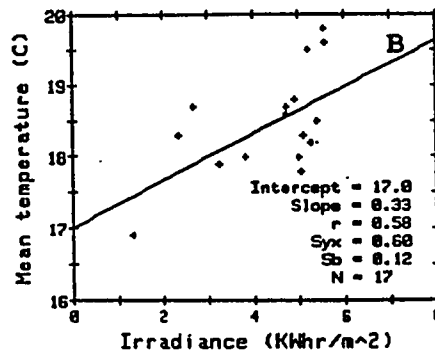
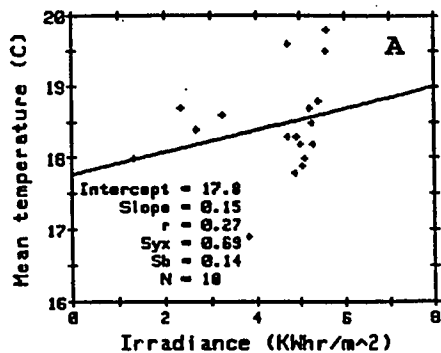


Figure 21. Correlation between daily solar irradiance with daily mean water temperature. A) Correlation with no lag. B) Correlation with solar irradiance lagged one day. C) Correlation between potential thermal heating with daily mean water temperature.

E_{total} is the solar broad band insolation, Z_{mean} is mean water depth, C_p is specific heat of water and d is water density. Based on the assumption that the South Marsh is uniformly 0.5 m deep and the temperature lag is removed, the water in the South Marsh warms up 0.2°C for each degree of potential thermal warming by solar insolation. These temperature observations indicate that as much as 20% of the daily solar broad band insolation may be absorbed by the water of the slough (Fig. 21C).

Tidal Currents

Tidal current measurements were taken to describe the current properties of Elkhorn Slough and to compare present day currents, at the slough entrance, with Clark's (1972) data to determine if the currents have changed. Currents in the slough were aligned with the channel axis as is characteristic of most narrow coastal inlets and estuaries. Current velocities were converted to their vector components, along-channel axis and cross-channel axis (Figs. 22 and 23). Positive values of along-channel velocity represent flood, and negative values represent ebb currents. Positive values of cross-channel velocity represent flow to the right and negative values represent flow to the left in the direction of flood currents. The relative magnitude of the cross-channel flow is insignificant, root-mean-square (RMS) values of 2.2, 2.9

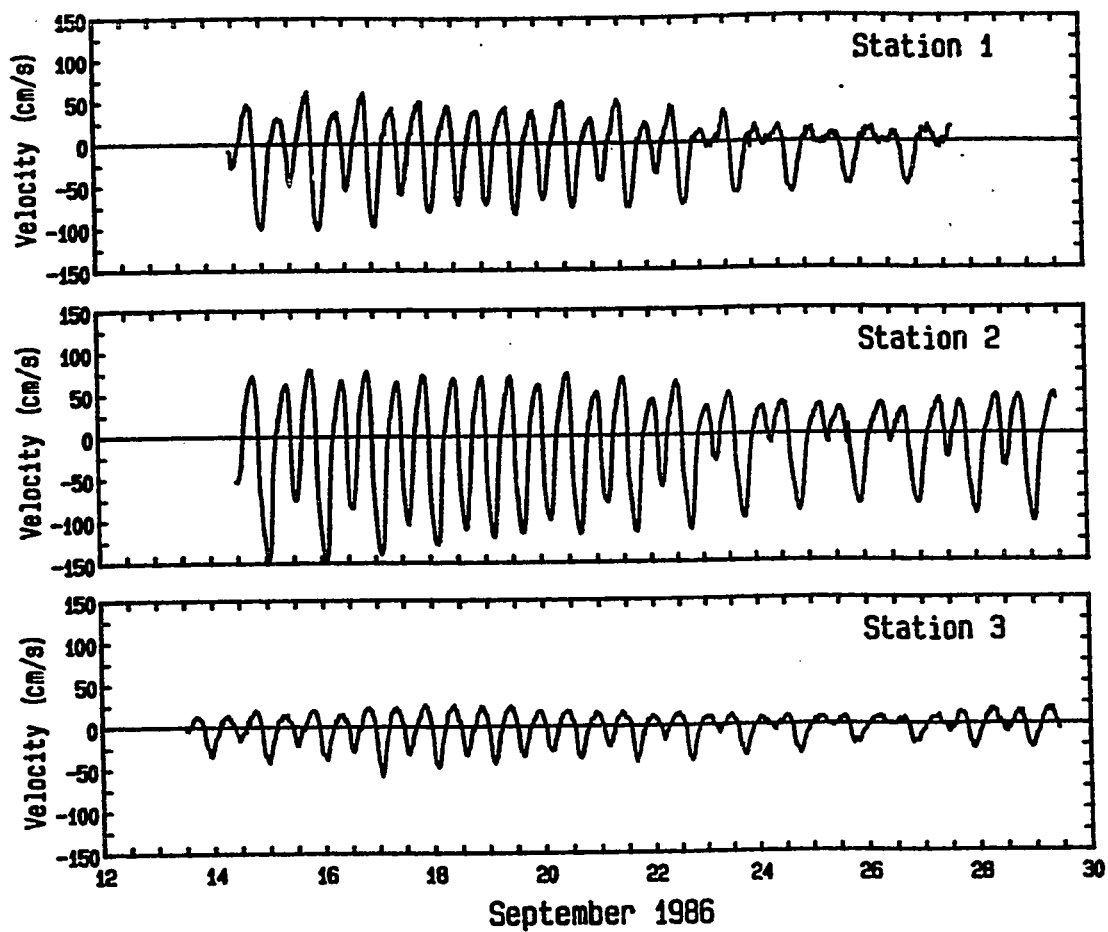


Figure 22. Time series of observed current velocity at stations shown in Fig. 7.

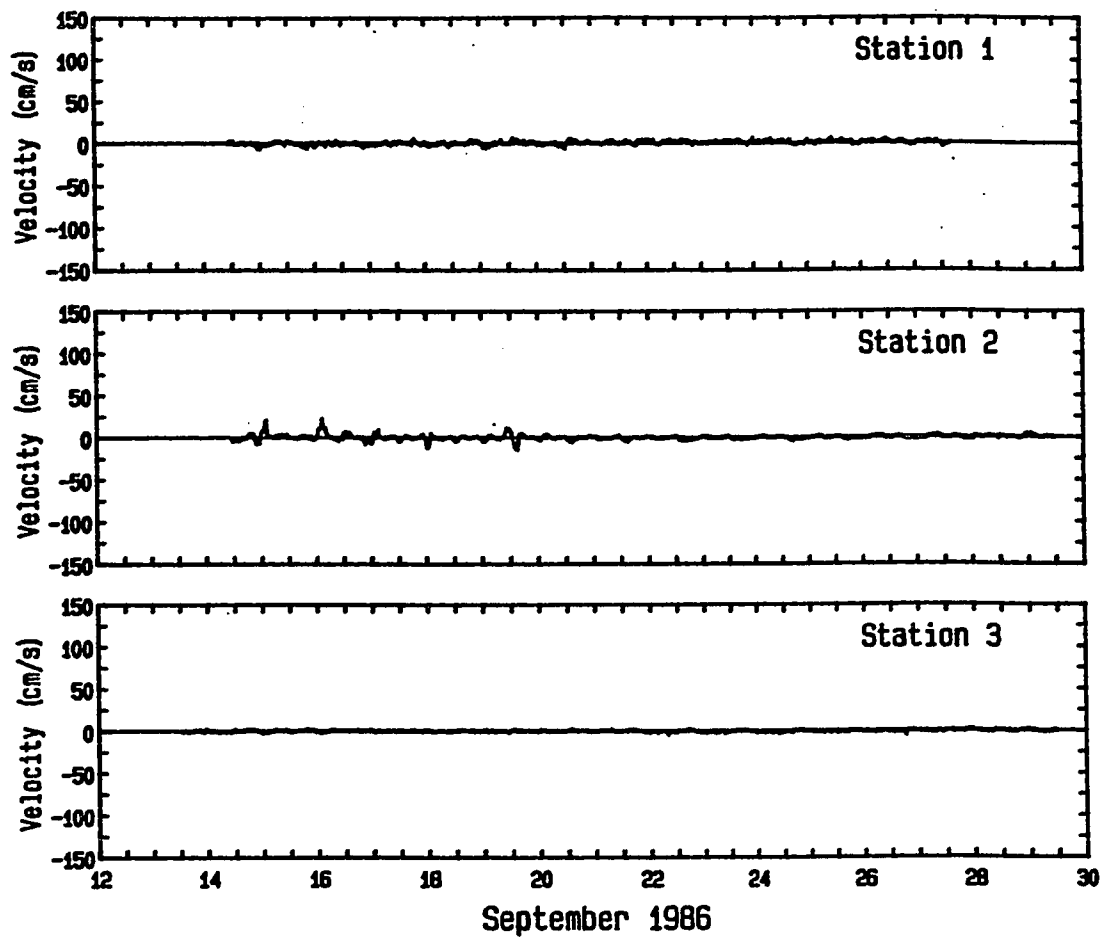


Figure 23. Time series of observed cross-channel current velocity at stations shown in Fig. 7.

and 1.0 cm/s (Fig. 23), compared to the along-channel RMS values of 29.6, 56.7 and 16.2 cm/s (Fig. 22).

Current velocities observed at the slough entrance were compared to Clark's (1972) station (slough entrance). He metered "free streaming" currents at mid-channel and mid-water depth, where the boundary friction effect is small. Current observations at station 1 were taken only 1.6 m above the bottom in 8 m of water, which is within the benthic boundary layer (Fig. 8A). Consequently, vertical profile measurements of currents were used (Fig. 24) to correct current velocity observations, taken in the boundary layer during September 1986, to "free streaming" velocities. These corrected values were then compared with Clark's data. These corrected values were also used to compute the sectional mean velocity to estimate volume transports, discussed later.

A logarithmic velocity distribution occurs in the boundary layer of tidal flows (Bowden, 1962; Ludwick, 1974; Sternberg, 1967). This distribution can be described using the Karman-Prandtl equation relating mean flow, U_z , at height Z , above the bottom, to boundary frictional stress:

$$U_z/U_* = 1/k \ln[(Z+Z_0)/Z_0], \quad (4)$$

where U_* is the frictional drag velocity, k is Von Karman's constant (approximately 0.4), and Z_0 is a roughness length.

Z_0 was computed by regressing observed current

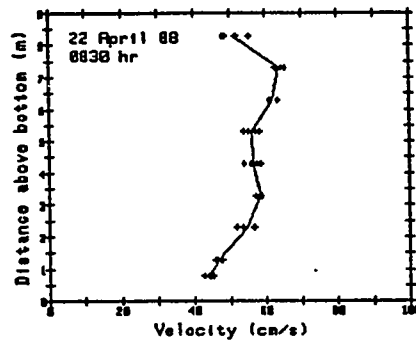
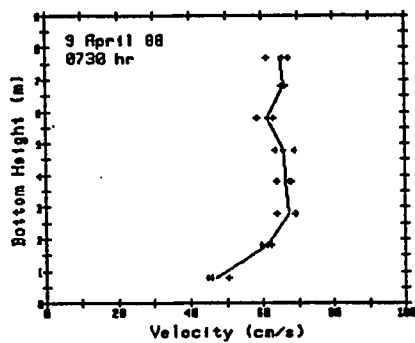
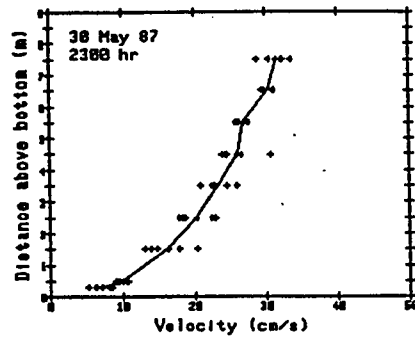
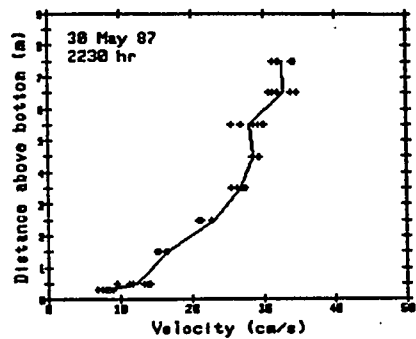


Figure 24. Vertical current velocity distributions from the bottom to the surface, at station 1. Vertical profiles observed at peak current flow.

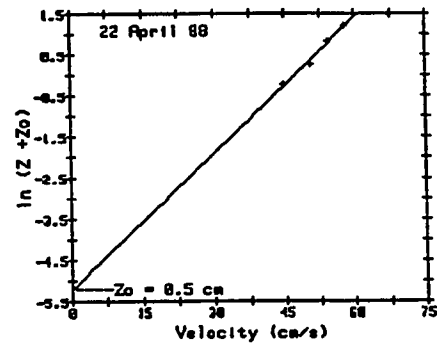
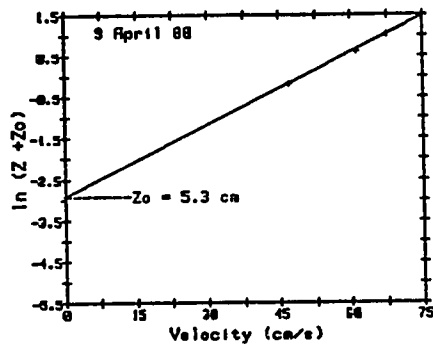
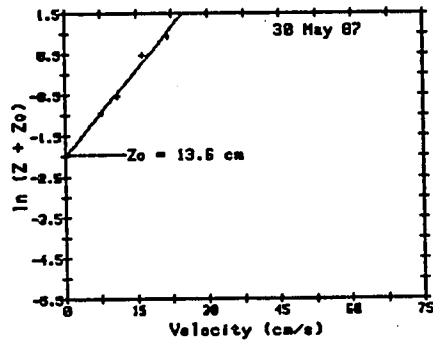


Figure 25. Determining roughness length, Z_0 , within the boundary layer, at station 1, from Inman (1963).

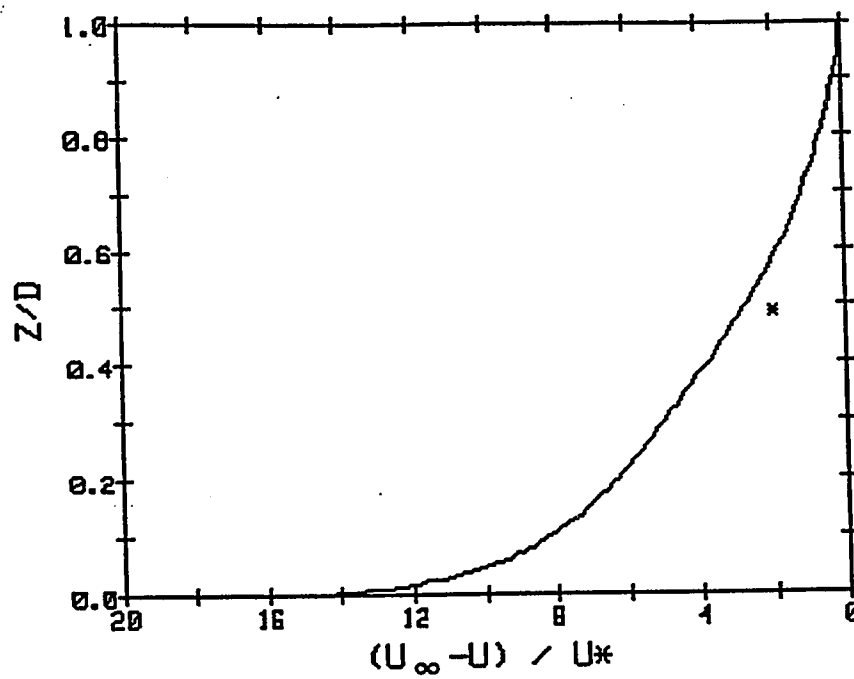


Figure 26. Comparison of the average velocity defect observed, at station 1, with the theoretical velocity defect distribution, from Komar (1976).

velocities in the estimated boundary layer against $\ln (Z)$. The ordinate axis intercept gives the first approximation of Z_0 . This value of Z_0 is entered in a second regression, velocities vs $\ln (Z + Z_0)$. The resulting value of Z_0 is considered to be the estimated roughness length (Inman, 1963) (Fig. 25). The average Z_0 in the bottom 3 m, at station 1, was 6.5 cm. The boundary layer velocity, U_z , was interpolated to the current meter moored height of 1.6 m and its average value was estimated to be 41.9 cm/s.

The values of U_z and Z_0 were entered into (4) to calculate an average U_* at the slough entrance. The calculated average U_* value of 4.4 cm/s appears to be a reasonable estimate compared to ranges of U_* , 2.4 to 4.5 cm/s, found in Puget Sound (Kackel and Sternberg, 1971), and 1.2 to 12.8 cm/s in Chesapeake Bay (Ludwick, 1974).

The computed mean value of U_* was then used to estimate the thickness of the boundary layer, D , using the velocity defect law (Komar, 1976):

$$(U_\infty - U_z) / U_* = -8.6 \log (Z/D), \quad (5)$$

where U_∞ is the mean velocity outside the boundary layer to the sea surface. From (5), the mean boundary layer thickness was estimated to be 3.3 m at the entrance.

The velocity defect, $(U_\infty - U_z) / U_*$, is correlated to the relative distance above the bottom within the boundary

layer. The mean value of U_z at station 1 is in fair agreement with the theoretical distribution (Fig. 26).

Equation 5 applies to boundary layer currents under steady unidirectional flow. Current observations, taken during September 1986, at station 1, varied over the tide cycle. To correct boundary layer observations to nonboundary layer velocities, the following assumptions were made: the boundary layer thickness and U_* remains constant throughout all tide phases and the mean varying nonboundary layer velocity, U , can be estimated by the ratio U_∞/U_z . The calculated ratio of U_∞/U_z , at station 1, was 1.21. All current velocity observations, at station 1, have been corrected to nonboundary layer velocities using this coefficient. Unless otherwise stated, all references to current velocities, at station 1 are corrected "free streaming" velocities. Current velocities observed at stations 2 and 3, which were near mid-depth, were assumed to be outside the boundary layer and were treated accordingly.

Table 9. Maximum observed current velocities during September 1986.

Station	Flood (cm/s)	Ebb (cm/s)	Date
1	53.1	- 85.2	15 September 1986
2	81.4	-153.6	15 September 1986
3	24.1	- 58.9	16 September 1986

Current observations indicate that the highest velocities occurred in the ebb direction at all stations (Fig. 22 and Table 9). Highest velocities were found at station 2 and lowest velocities took place at station 3 (Table 9) and coincided with the larger semidiurnal tidal ranges (Figs. 13 and 22). Spectral analysis showed that semidiurnal and diurnal tidal forcing was responsible for 92 to 96% of the total current velocity variance (Fig. 27).

Flood and ebb current did not simply reverse directions by 180° as would be expected for current flow in a long straight channel. Elkhorn Slough is composed of meandering channels, typical of tidal lagoons, estuaries and rivers. As water flows around a bend the outer bank deflects water flow and changes the direction of flow, while centripetal acceleration causes currents in the outer loop of the bend to move faster than currents in the inner loop. If currents are metered near a channel bend, the change in current direction will be metered in water flow following the bend but will not be affected by flow in the opposite direction. In addition, if currents are metered along the outer loop, the centripetal acceleration of currents will only be observed in the channel flow after the bend. This shape effect was likely observed at each meter station since the reverse in tidal currents did not simply change direction by 180° , and channel bends are present near each station. The directional shape effect

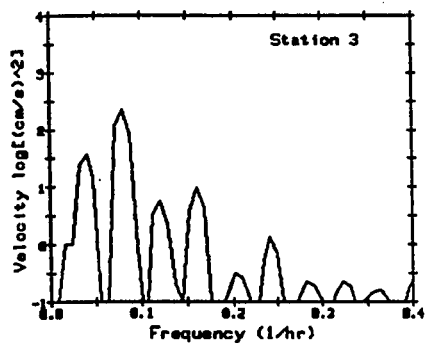
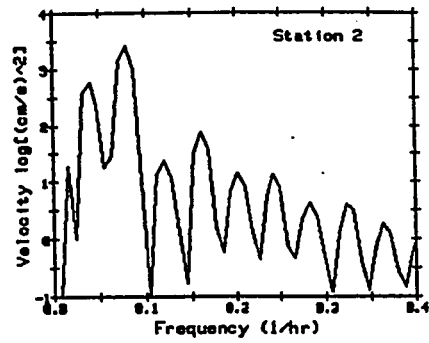
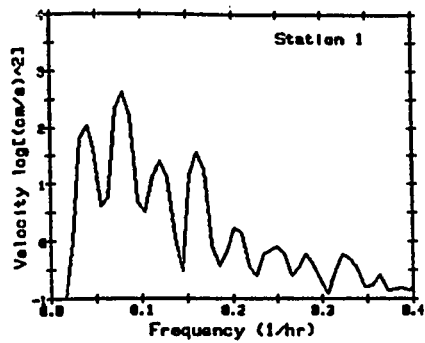


Figure 27. Current velocity spectra for stations shown in Fig. 7.

was removed during calculation of the along-channel and cross-channel vectors.

Highest current velocities were in the ebb direction of Elkhorn Slough (Table 9). The maximum ebb velocity during September 1986 was about twice as high as the flood velocity. A higher maximum ebb velocity was consistent with an ebb dominant estuary as described by Friedrichs and Aubrey (1988) for the U.S. east coast, where ebb tides have higher currents and shorter durations than flood tides. However, on the U.S. west coast, including Elkhorn Slough, mixed semidiurnal tides are prevalent. A characteristic of mixed tides, in Elkhorn Slough, is that the greatest tidal range usually occurs from higher high water to lower low water. Highest current velocities were observed during this period. Although the duration of diurnal flood tides was longer than ebb tides, higher ebb velocity is as much a function of a larger ebb tidal range as the asymmetric tide resulting from tidal flats. Because tides on the U. S. west coast are mixed, maximum velocity of flood and ebb currents may not be as useful a criterion in classifying tidal embayments as flood or ebb dominant systems along the west coast of the United States.

Tides may exhibit standing wave and progressive wave characteristics. A feature of a pure standing wave tide is that maximum currents occur midway between the time of high and low water. In contrast, maximum flood and ebb currents

in progressive wave tides coincide with high and low water. Tidal currents in Elkhorn Slough are mixed in this regard: the average time of maximum current speed generally occurred during the latter half of the half-tidal cycle for all stations (Table 10).

Table 10. Mean duration of rising and falling water and mean lag time to maximum current velocity, during September 1986.

Period	1		Station 2		3	
	Time (hr)	std. dev. (hr)	Time (hr)	std. dev. (hr)	Time (hr)	std. dev. (hr)
<u>Flood</u>						
duration	6.4	1.0	7.1	0.7	7.0	0.9
lag	5.1	1.1	5.2	0.8	3.8	1.1
<u>Ebb</u>						
duration	6.0	1.8	5.4	1.6	5.5	1.8
lag	3.0	1.1	3.8	1.1	2.3	0.7
<u>Combined</u>						
duration	6.2	1.4	6.2	1.5	6.2	1.6
lag	4.0	1.5	4.1	1.4	3.0	1.1

The time of maximum flood velocity was shifted towards the time of high water, while the time of peak ebb velocity was shifted slightly later or occurred midway through the ebb tide (Fig. 28). Tidal flats are probably responsible for the long lag of maximum flood velocity from the time mid-way between high and low water. When the rising tide reaches the elevation of the tidal flats, an increase in current speed is required to move enough water volume to

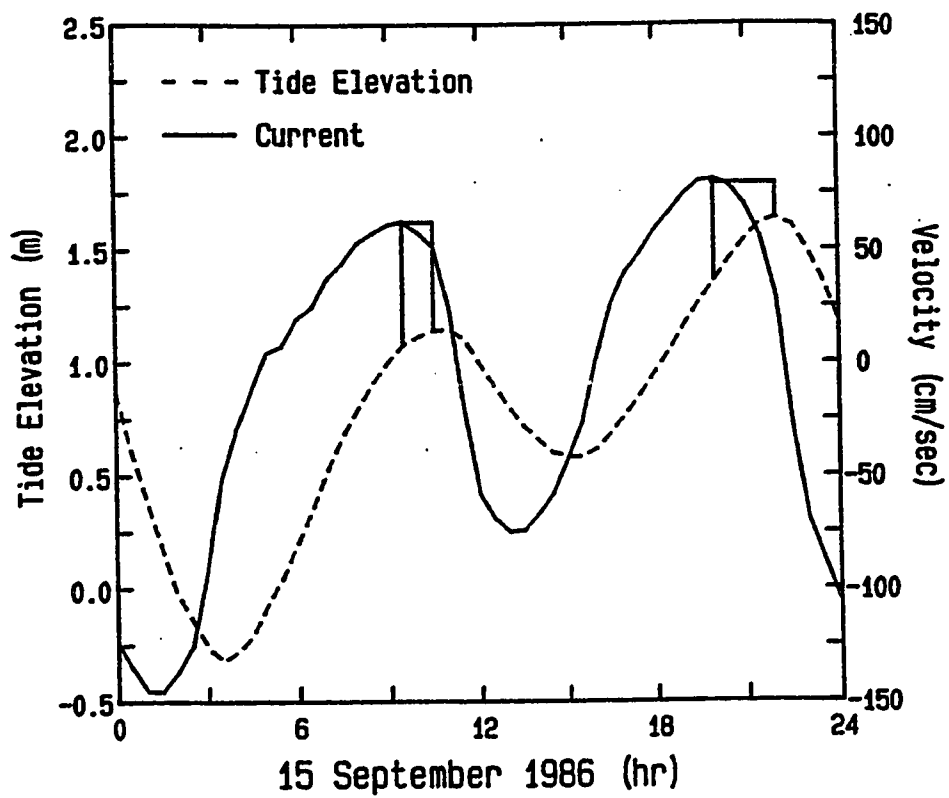


Figure 28. Current velocity and tidal elevation at station 2 on 15 September 1986. Note that the time of maximum flood current velocity is shifted towards the time of high tide.

fill the expanded area over the tidal flats. This generally happens during the latter half of the flood tide cycle, and causes the time of maximum flood current velocity to occur up to 1.9 hr later than the midpoint of the half-tide cycle (Table 10). However, during the ebb tide, water over the tidal flats is able to flow seaward immediately after the tide reverses; this reduces the lag of maximum ebb velocity from the midpoint of the half-tide cycle.

Maximum currents are not solely a function of tidal range because of variations in the duration of flood or ebb tides over the same tidal range. Sverdrup et al. (1942) have related maximum current velocity, U , at a particular channel location to its basin geometry by:

$$U = 4/3 * \pi/2 * A/S * H/T \quad (6)$$

where U is the maximum tidal velocity over the half-tidal period, $4/3$ relates the cross-sectional mean velocity to the mean mid-channel velocity, $\pi/2$ relates the mean velocity of the half-tidal period to the maximum half-tidal velocity, H is the half-tidal range, A is the surface area of the basin, S is the cross-sectional area, and T is the duration of the half-tide period. Equation 6 states that tidal currents in a channel are proportional to the surface area of the basin and the range of the tide, but inversely proportional to the cross-sectional area and half-tidal

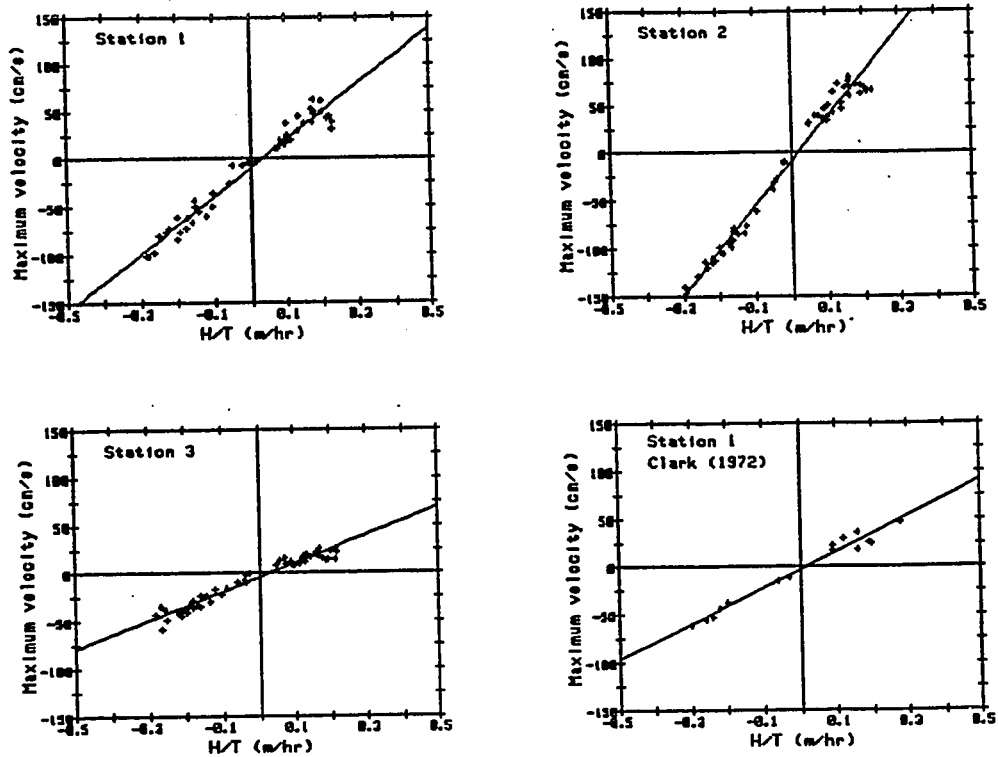


Figure 29. Least squares regression of maximum current with tide height rate of change, at stations shown in Fig. 7 and Clark's (1972) Highway 1 Bridge station.

period. Assuming constant basin shape and cross-sectional area, tidal currents are directly related to the water level's rate of change during a half-tide cycle, H/T . Clark used (6) in a least squares regression model to describe maximum current velocity at the mouth of Elkhorn Slough (Fig. 29).

The regression model can be used to describe three parameters of the slough. The intercept gives an indication of the net nontidal currents, the slope gives an estimate of the geometry of the slough and the summation of the area, based on slough geometry, and tidal height gives the volume of the slough.

Table 11. Statistics of least squares regression of maximum current velocity vs H/T for stations 1, 2, 3 and Clark's (1972) station.

Station	Regression	r	Statistics			N
			S_{yx}	S_b		
1	$V_{max} = -9.6 + 297 H/T$	0.96	9.7	8.1		51
2	$V_{max} = -8.9 + 463 H/T$	0.98	10.3	8.3		56
3	$V_{max} = -4.5 + 148 H/T$	0.95	5.4	4.4		59
Clark's data	$V_{max} = -3.1 + 187 H/T$	0.97	6.4	6.4		15

The intercept of the regression of maximum current velocity over the half-tidal period against H/T suggests a nontidal seaward flow from Elkhorn Slough at all stations (Table 11). Sources that might contribute to nontidal currents include: agricultural inflow, evaporation, pumping

by P.G. & E., rain runoff and measurement bias. Agricultural inflow is estimated to be $2 \times 10^6 \text{ m}^3/\text{day}$ (Water Resources Engineers, 1969). Evaporation from Elkhorn Slough for the month of September is estimated to be about $1 \times 10^4 \text{ m}^3/\text{day}$ and would cause a net landward flow (Smith, 1972). P.G. & E. discharges approximately $4 \times 10^5 \text{ m}^3$ of coolant water into Elkhorn Slough per day (Ecological Analysts, Inc., 1983) and the net seaward flow observed by Clark at station 1 was attributed to P.G. & E.'s discharge. However, this source would not contribute to a seaward flow at stations 2 and 3. A mean daily volume exchange in Elkhorn Slough of $11.4 \times 10^6 \text{ m}^3$ (see volume exchange) is 2 to 3 orders of magnitude greater than agricultural runoff or evaporation. The total daily P.G. & E. discharge amounts to 4% of the mean daily volume exchange and can account for 1.7 cm/s of the apparent total nontidal outflow of slough water at station 1.

A storm dropped 4 cm of rain into the slough area from 23 through 27 September 1986 (Melaine Munk, Watsonville Register Pajaronian, pers. comm.). The drainage basin of the Elkhorn Slough area is 585 km^2 , giving a potential inflow $2.3 \times 10^7 \text{ m}^3$ of water over the five day period of precipitation, or an average of $4.6 \times 10^6 \text{ m}^3/\text{day}$, which is about half of the daily mean tidal prism. Factors such as the infiltration of rain water, uneven precipitation, water diversion within the

drainage basin and evaporation make it difficult to estimate the impact of rain on the slough's hydrography. There was no noticeable change in the data for tides or currents (Figs. 13 and 22). However, it is probably safe to assume that rainfall did contribute to a net seaward flow after 24 September and continued to be some factor until the end of the time series.

Another source of an apparent net transport out of Elkhorn Slough may be attributed to shape effect of the channel discussed previously. Since each station was situated along the outer bank of a bend relative to the ebb flow, the centripetal acceleration resulting from the channel bend, may have been measured as a seaward current, causing an apparent net nontidal ebb flow. Whatever the source of the apparent net nontidal seaward flow, its magnitude is within the standard error of the estimate (Table 11) and is not statistically different than zero at all stations. Therefore, the net transport may or may not be real. Since nontidal currents seem to have been found at all stations over both studies, this may be a subject for further investigation.

A comparison of current velocities between station 1 and data collected by Clark indicated that the velocities at the entrance of Elkhorn Slough have increased approximately 55% since Clark's observations (Fig. 29). This is indicated by an increase of the regression slope

from 187, for Clark's data, to 297 cm·hr/m·s for the present study (Table 11). A t-test showed that the slopes were significantly different ($P < 0.001$). The slope of maximum velocity vs H/T represents the ratio of the "effective surface area" of the embayment to cross-sectional area of the channel, A/S. When the channel is enlarged, such as by dredging, the cross-sectional area is increased and current velocities decrease. However, when the effective surface area of the embayment is increased, such as in the restoration of former wetlands to Elkhorn Slough, current velocities increase. The observed increase in current velocities at the entrance of the slough is compelling testimony of a significant expansion of tidally influenced lands within the Elkhorn Slough system since Clark's study.

Clark (1972) suggested that the highest current velocity, at the slough entrance, should occur during the December spring tides with an expected tidal range of 2.5 m over a 7.2 hour half-tidal period, which corresponds to an H/T equal to -0.35 m/hr for an ebb tide. He predicted a maximum ebb current of -72 cm/s (1.5 kt) and a maximum flood current of 60 cm/s, at the slough entrance. Results from this study show that the maximum predicted velocities have changed: maximum ebb velocity is now -113 cm/s (2.3 kt) and maximum flood velocity is 94 cm/s (1.9 kt).

The maximum currents at station 2 were 55% higher than

at station 1. The higher velocities observed at station 2 can be accounted for by the relatively large water volume that must be funneled through a small channel area (Fig. 7). The predicted maximum velocities, at station 2, would be -171 cm/s (3.4 kt) and 153 cm/s (3.1 kt). Station 3 velocities were 50% lower than at station 1. Since the channel is wide relative to the discharge volume, it is reasonable to expect significantly lower current velocities at this location. The maximum expected velocities, at station 3, are -56 cm/s (1.1 kt) and 47 cm/s (0.9 kt).

The linear model (6) used to describe maximum velocity vs H/T is only accurate to describe a channel of uniform shape. In such a channel, maximum current velocity is directly proportional to the change in tidal height. Adding tidal flats to the channel area would change the shape of the regression curve when tide level reaches tidal flat elevation. This change occurs because friction over the tidal flats does not allow for effective water transport. Thus, current velocity in the channel must increase to compensate for the increase in volume transport within the channel boundaries. Maximum velocity is no longer directly proportional to H/T and the relationship between current velocities vs H/T becomes nonlinear. Tidal flats are located along the slough's middle and upper reaches at approximately mean sea level. Consequently, the

relationship between maximum velocity and H/T is not entirely linear. The error involved in using a linear equation to model Elkhorn Slough currents is that velocities may be over-estimated during large tidal ranges and under-estimated during small tidal ranges.

Effective Surface Area and Volume Transport

Clark calculated the "effective surface area" of Elkhorn Slough by:

$$A = S * (3/4 * 2/\pi * b), \quad (7)$$

where b is the least squares slope from (6) (Fig. 29 and Table 11). The effective surface areas of the slough inland to each station were calculated using this method (Table 12). A comparison of the slough's change in effective surface area indicates that the low tide (0.0 m) area covered by water has increased from 1.1 to 2.1 km² and the mean high tide (1.5 m) area from 1.5 to 3.1 km². The maximum effective surface area covered by water on the highest tide (2 m) is now 3.5 km².

Water volume was computed as a function of tidal height, H and effective surface area, A (Table 12):

$$V = H * A.$$

These values were compared to cumulative volume estimates made by Smith (1972). He estimated the cumulative slough

Table 12. Cumulative surface area and volume estimates, derived from maximum current velocity observations.

Tide Height (m)	1		Station 2		3	
	A	V	A	V	A	V
2.0	3.5	10.0	1.3	3.3	1.1	3.3
MHHW 1.7	3.3	9.0	1.2	2.7	1.0	2.8
1.5	3.1	7.8	1.1	2.2	0.9	2.3
MSL 1.0	2.7	5.4	0.9	1.4	0.6	1.2
0.5	2.4	3.6	0.7	0.7	0.5	0.8
MLLW 0.0	2.1	2.1	0.6	0.3	0.3	0.3
-0.5	1.9	0.9	0.5	<0.1	0.2	0.1

$$\text{Area} = A \times 10^6 \text{ m}^2$$

$$\text{Volume} = V \times 10^6 \text{ m}^3$$

Assumptions:

Main channel effective water depth at MLLW = 1 m.

SM/PS effective water depth at MLLW = 0.5 m.

volume as the product of water height and the area over the channel, mud flat and marsh. The area of water coverage over the channel, mud flat and marsh was estimated by planimetry of an Elkhorn Slough map (drawn by John C. Hansen). The idealized cross sectional geometry (Fig. 6) was used to estimate water height over each section. For this study, the effective MLLW depth for the entire slough, including SM/PS, was estimated to be 1 m. Consequently, the volume at MLLW is estimated to be $2.1 \times 10^6 \text{ m}^3$, which is only 5% greater than the $2.0 \times 10^6 \text{ m}^3$ estimated by Smith. However, the mean diurnal high tide volume has increased from 6.0×10^6 to $9.0 \times 10^6 \text{ m}^3$. The mean tidal prism has enlarged from 4.0×10^6 to $6.9 \times 10^6 \text{ m}^3$ and total cumulative water volume of Elkhorn Slough on the highest

tide has grown from 8.5×10^6 to $10.0 \times 10^6 \text{ m}^3$.

The mean diurnal tide, (0.0 to 1.7 m) flushes approximately 75% of the total volume out of the slough. This is about the same proportion of flushing observed by Smith. Considering Smith's assumption that the remaining slough water mixes insignificantly with incoming Monterey Bay water, the tidal prism would extend 4.8 km inland, which is just beyond the entrance to SM/PS. After the restoration of former wetlands to tidal circulation the proportion of tidal flushing remains virtually unchanged. Smith's observation of a foam line introduced from the P.G. & E. discharge appearing 4 to 5 km inland is still observed today.

It is interesting to note that the effective surface area has essentially doubled since Clark's study in 1972, but the low tide volume has remained about the same as shown by Smith for 1974. Enlargement of the channels by erosion, since 1974, should have increased the low tide volume. Because of imperfections in both models used, it is difficult to ascertain which model is in greater error. However, a 50% increase in diurnal high tide volume, including SM/PS, since 1974, appears to be reasonable estimate for the entire Elkhorn Slough system.

Comparison of volume capacity calculated at stations 1 through 3 (Table 12) indicates that the upper slough and SM/PS contain approximately equal water volume. At low

tide, 70% of the total volume is concentrated in the lower slough while remaining 30% is divided equally between the upper slough and SM/PS region. At mean diurnal high tide, the lower slough volume drops to 40% as the holding capacity of the upper slough and SM/PS regions increase dramatically with infilling over the tidal flats. Approximately 30% of the slough volume is held in the upper slough and about 30% of the volume is present in the SM/PS region at mean diurnal high tide.

Volume transports through each station section were also calculated using an integrated volume transport model over a half-tide cycle. The exchange volume was estimated by integrating the mean cross-sectional velocity, U_c , and the cross-sectional area of the channel, S , over time a half-tidal cycle (Hansen, 1965):

$$V = \int_{\text{low}}^{\text{high}} U_c * A(t) dt, \quad (8)$$

where V is the half-tide exchange volume and t is time.

Volume transports for each half-tide cycle were regressed against tidal range to produce a tidal prism model (Fig. 30). Similar to the maximum velocity analysis, the volume transport regressions resulted in negative intercepts indicating a net nontidal transport seaward at each station. The apparent nontidal flow of water from the slough, at station 1, is $4.9 \times 10^5 \text{ m}^3$ per semidiurnal tide. The P.G. & E. semidiurnal discharge of $2 \times 10^5 \text{ m}^3$ into

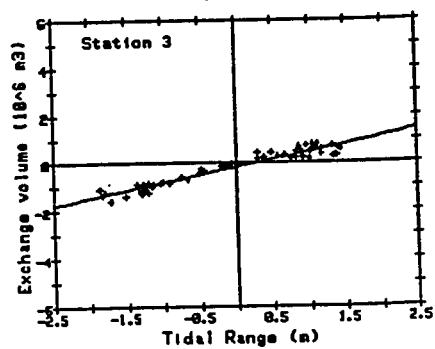
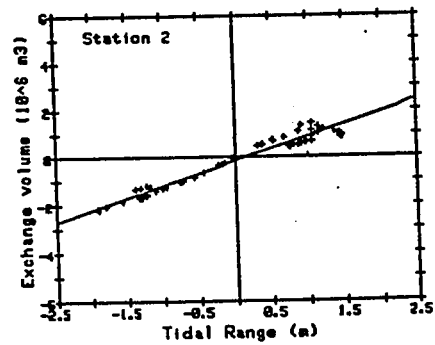
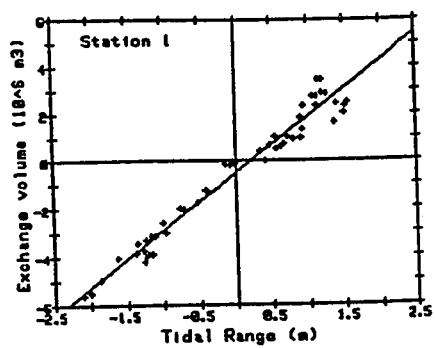


Figure 30. Least squares regression of exchange volume with tidal range at stations shown in Fig. 7.

Elkhorn Slough accounts for about 40% of this nontidal flux and 1.7 cm/s of the nontidal ebb flow, at station 1. Since the volume exchange calculations are linked to tidal velocity measurements, they are affected by the same sources of error. As with the velocity calculations, the magnitude of the nontidal transport cannot be statistically differentiated from zero (Table 13). Thus the intercept was adjusted to reflect zero nontidal transport for calculations using this model.

Table 13. Statistics of least squares regression of exchange volume vs tidal range for stations 1, 2 and 3, based on the integral method.

Station	Regression	r	Statistics		N
			S _{yx}	S _b	
1	V = -0.5 + 2.4 * R	0.98	0.51	0.07	51
2	V = -0.1 + 1.0 * R	0.98	0.23	0.03	56
3	V = -0.1 + 0.6 * R	0.96	0.19	0.02	59
V = exchange volume (10 ⁶ m ³)					
R = tidal range (m)					

The mean diurnal tidal prism calculated by the integral technique was $3.6 \times 10^6 \text{ m}^3$ and the tidal prism for an extreme spring tide of 2.5 m was $5.9 \times 10^6 \text{ m}^3$. The mean exchange volumes calculated by the integral method were 35% less than the volumes calculated from (6), at station 1 (Tables 12 and 14). Compared to (6), the integral method under-estimated volume transport by 20% at station 2 and 50% at station 3. The linear integral model relating the

Table 14. Exchange volume calculated by the integrated volume transport method.

Tide Range (m)	Station		
	$\frac{1}{V}$	$\frac{2}{V}$	$\frac{3}{V}$
2.5	5.9	2.6	1.6
2.0	4.8	2.1	1.3
1.5	3.6	1.6	1.0
1.0	2.4	1.1	0.7
0.5	1.2	0.6	0.4
Exchange volume = $V \times 10^6 \text{ m}^3$			

slough's exchange volume directly to the change in tidal range is probably not appropriate in Elkhorn Slough, where the channel geometry changes at mud flat elevation. A nonlinear geometry combined with mixed semidiurnal tides caused large differences in volume transport estimates over the same tidal range depending on whether the transport transpired above or below the tidal flat elevation.

Poor accuracy in referencing pressure observations to MLLW may have contributed to part of the discrepancy between the two methods of estimating volume exchange. But the greatest error in (6) and (8) stems from the deployment of only one current meter at each station, giving a poor estimate of the true cross-sectional mean velocity. Acquiring accurate volume transport estimates using more current meters per station is a project worthy of further study. Despite the difficulty in calculating volume estimates, the lower transports calculated by (8) is

Table 15. Cumulative surface area of South Marsh and Parson Slough, derived from planimetered data.

Location	<u>Channel area</u>	<u>Tidal Flat area</u>
	A	A
South Marsh	0.2	0.7
Parson Slough	0.1	1.1
SM/PS	0.3	1.8
Cumulative surface area = $A \times 10^6 \text{ m}^2$		

Table 16. Volume estimate of South Marsh and Parson Slough, derived from planimetered cumulative surface areas.

Tide Height (m)		Location		<u>Total SM/PS</u> V
		<u>SM</u> V	<u>PS</u> V	
MHHW	2.0	1.2	1.4	2.6
	1.7	1.0	1.2	2.2
	1.5	0.9	0.9	1.7
MSL	1.0	0.5	0.3	0.8
	0.5	0.4	0.2	0.6
MLLW	0.0	0.3	0.1	0.4
	-0.5	0.2	0.1	0.2

$$\text{Volume} = V \times 10^6 \text{ m}^3$$

Assumptions:

Tidal flat elevation = 0.9 m.

Effective MLLW depth = 0.75 m.

an indication that the estimated slough volume and volume exchange derived from (6) may be over-estimated.

Cumulative water volume for the SM/PS region was independently calculated from planimetered data off an aerial photograph similar to figure 31. The product of the digitized area (Table 15), using the idealized slough



Figure 31. Aerial photograph of Elkhorn Slough, at low tide on 19 May 1983. Scale = 1:24000.

geometry (Fig. 6), and tidal height were used to calculate total water volume in SM/PS over the full tidal range (Table 16). The planimetered total volume estimates for SM/PS were as much as 50% greater at lowest tide (-0.5 m) and 20 % smaller at highest tide (2 m) than estimates derived by (6) (Tables 12 and 16). This discrepancy in volume estimate also indicated that the linear model used to estimate water volume in Elkhorn Slough may be over-estimating high tide volumes and under-estimating low tide volumes. In the final analysis, the estimates derived by (6) appear to be high compared to the values derived by (8), and the planimetered method gives estimates that fall somewhere between these two methods. The planimetered technique is probably the most accurate and volume estimates for the entire slough likely falls somewhere between the values derived by (6) and (8).

CONCLUSIONS

The restoration of former wetlands has increased the tidal flat area and altered the tidal characteristics of Elkhorn Slough. Distortion of the oceanic semidiurnal tide period is evident in longer durations of rising water. This feature has become more pronounced since the restoration of wetlands and has increased the phase lag of high tide. The high tide phase lag is produced when a large volume of water is transported across the tidal flat, late in the flood cycle. Therefore, it takes longer to fill the slough than if the additional areas at tidal flat elevation were not present. Because most of the volume transport takes place during the later part of the flood cycle, the time of maximum current is also shifted to the later half of the flood period. Tide asymmetry may be represented by the generation of shallow water constituents, M_4 , MK_3 and $2MK_3$.

Water temperature in the channel varies inversely with the semidiurnal tide illustrating the removal of warm water out of the slough and the introduction of cold Monterey Bay water returning into the slough. Diurnal variation in water temperature at the head of the South Marsh indicates a lower turnover rate for areas in the upper reaches of the Research Reserve and an estimated transfer of 20% of the solar insolation to thermal heating of slough water.

Semidiurnal and diurnal tidal forcing was responsible for 97 to 99% of the variance in Elkhorn Slough currents. Current velocities at the entrance of the slough have increased by 55% since Clark's (1972) study. Most of this increase in tidal flow is due to slough restoration, while some of the increase may be attributed to slough erosion. The highest expected velocity at the entrance of Elkhorn Slough is estimated to be 94 cm/s (1.9 kt) on a flood tide and -113 cm/s (2.3 kt) on an ebb tide. Higher maximum ebb velocity in conjunction with longer flood durations are the criteria used in classifying Elkhorn Slough as an "ebb dominant" system. Although ebb dominant embayments are normally described as stable systems, Elkhorn Slough has and is still experiencing significant erosion, caused by high current velocities. Addition of more land to tidal circulation will likely prolong or increase erosion.

The "effective surface area" has apparently doubled over Clark's estimates. The cumulative mean diurnal volume and tidal prism have expanded 50% and 70% over Smith's estimates, respectively. The ratio of the tidal prism to high tide volume remains about the same as earlier estimates, at approximately 3/4 of the mean high water volume. The upper slough and SM/PS regions hold approximately equal volumes of water. At low tide the lower slough held 70% of the cumulative water volume. However, lower slough volume decreased to 40% of the total

volume at diurnal high tide after water fills the tidal flats in the SM/PS and along the upper slough regions.

The intentional and accidental restoration of former wetlands to tidal circulation has not only directly expanded the area and volume of tidally influenced lands, but has indirectly contributed to the expansion of Elkhorn Slough through erosion caused by increased tidal currents. The erosion process was initiated by the opening of a permanent harbor channel at the entrance of Elkhorn Slough in the 1940's. It is likely that the channel area will continue to widen and deepen, even if no additional former wetlands are returned to tidal circulation. In view of the erosion caused by tidal currents, it might be advisable to conduct a quantitative study of sediment transport before further alterations to the Slough are considered.

REFERENCES

- Aubrey, D. J. and P. E. Speer. 1985. A study of non-linear tidal propagation in shallow Inlet/Estuarine Systems Part I: Observations. *Estuarine, Coastal and Shelf Science*. 21:185-205.
- Boon, J. D. and R. J. Byrne. 1981. On basin hypsometry and the morphodynamic response of coastal inlet systems. *Marine Geology*. 40:27-48.
- Bowden, K. F. 1983. *Physical Oceanography of Coastal Waters*. John Wiley and Sons, New York. 302 p.
- Broenkow, W. W. and R. E. Smith. 1972. Hydrographic observations in Elkhorn Slough and Moss Landing Harbor, Calif., October 1970 to November 1971. Moss Landing Marine Laboratories Tech. Pub. 72-3. 74 p.
- Browning, B. M. 1972. The Natural Resources of Elkhorn Slough, Their Present and Future Use. Calif. Dept. Fish and Game, Coastal Wetland Series No 4. 105 p.
- Clark, L. R. 1972. Long Period Wave Characteristics in Moss Landing Harbor and Elkhorn Slough. M. A. Thesis, Natural Sci. Dept., Calif. State Univ., San Jose. 73 p.
- Conomos, T. J. 1979. Properties and Circulation of San Francisco Bay Waters. In: *San Francisco Bay. The Urbanized Estuary*. Pacific Div. American Assoc. for Adv. of Sci. San Francisco, Calif. p. 47-84.
- Defant, A. 1964. *Ebb and Flow*. University of Michigan Press. Ann Arbor, Michigan. 121 p.
- Doodson, A. T. and H. D Warburg. 1952. *Admiralty Manual of Tides*. Her Majesty's Stationary Office. Hydrographic Dept. Admiralty, London, Eng. 270 p.
- Dyer, K. R. 1973. *Estuaries: A Physical Introduction*. John Wiley & Sons. New York, N. Y. 140 p.
- Ecological Analysts, Inc. (EA). 1983. Moss Landing Power Plant Cooling Water Intake Structures 316(b) Demonstration. Prepared for Pacific Gas and Electric Company, San Francisco. 413 p.

- Friedrichs, C. T., and D. G. Aubrey. 1988. Non-linear tidal distortion in shallow well-mixed estuaries: a synthesis. *Estuarine, Coastal and Shelf Science*. 27:521-545.
- Gartner, J. W., and R. Oltmann. 1985. Comparison of Recording Current Meters Used for Measuring Velocities in Shallow Waters of San Francisco Bay, California. *Ocean Engineering and the Environment* conference record; November 12-14, 1985: Joint conference of Marine Technology Society and IEEE Ocean Engineering Society. p. 731-737.
- Gordon, B. L. 1977. Monterey Bay area: natural history and cultural imprints. 2nd ed, Boxwood Press. Pacific Grove, Calif. 321 p.
- Hansen, D. V. 1965. Currents and Mixing in the Columbia River Estuary. *Ocean Science and Ocean Engineering: Joint Conference of Marine Technology Society and American Society of Limnology and Oceanography*. Wash., D. C., June 1965. p. 943-955.
- Inman, D. L. 1963. Sediments: Physical properties and mechanics of sedimentation. *In*: F. P. Shepard (ed.), 2nd ed. *Submarine Geology*. New York, N. Y. p. 101-151.
- Jenkins, O. P. 1974. Pleistocene Lake San Benito: California. *Geology*, July. p. 151-163.
- Kachel, N. B. and R. W. Sternberg. 1971. Transport of Bedload as Ripples During an Ebb Current. *Marine Geology*. 10:220-244.
- Knauss, J. A. 1978. Introduction to Physical Oceanography. Prentice Hall, Inc. Englewood Cliffs, New Jersey. p. 220-241.
- Komar, P. D. 1976. Boundary Layer Flow Under Steady Unidirectional Currents. *In*: Stanley, D. J. and D. J. P. Swift (ed.). *Marine Sediment Transport and Environmental Management*. John Wiley and Sons. New York, N. Y. p. 91-125.
- Ludwick, J. C. 1974. Tidal Currents and Zig-Zag Sand Shoals in a Wide Estuary Entrance. *Geological Society of American Bulletin*. 85:717-726.

- MacGinitie, G. E. 1935. Ecological aspects of a California Marine Estuary. *Am. Midl. Nat.* 16(5):629-765.
- Martin, B. D. 1964. Monterey Submarine Canyon: California: genesis and relationship to continental geology Ph.D. dissertation, Univ. of So. Calif. Geology Dept. Los Angeles, Calif. 194 p.
- Monterey Bay Aquarium & Moss Landing Marine Laboratories
Monthly Weather and Oceanographic Summary. Sept. 1986.
- NOAA Tide Tables. 1986. West Coast on North and South America. National Oceanic and Atmospheric Administration. U. S. Dept. of Commerce. Wash., D. C. 234 p.
- Nybakken, J., G. Caillet and W. Broenkow. 1977. Ecologic and Hydrographic studies of Elkhorn Slough Moss Landing Harbor and Nearshore Coastal Waters. Moss Landing Marine Laboratories. Moss Landing, Calif. p. 397-465.
- Pond, S. and G. L. Pickard. 1983. Introductory Dynamical Oceanography. Pergamon Press, New York, N. Y. 329 p.
- Redfield, A. C. 1980. Introduction to Tides. The Tides of the Waters of New England and New York. Marine Science International. Woods Hole, Mass. 108 p.
- Reilly, P. T. 1978. Phosphate Flux in Elkhorn Slough: California. M. A. Thesis, Natural Sci. Dept., Cal. State Univ., San Jose. 80 p.
- Schureman, P. 1971. Manual of Harmonic Analysis and Prediction of Tides. United States Gov. Printing Office. U. S. Dept. of Commerce Pub. 98. Wash., D. C. 317 p.
- Schwartz, D. L. 1983. Geologic History of Elkhorn Slough, Monterey County, California. M. S. Thesis, Geology Dept., Cal. State Univ., San Jose. 102 p.
- Smith, R. E. 1974. The Hydrography of Elkhorn Slough, A Shallow California Coastal Embayment. M. A. Thesis, Natural Sci. Dept., Calif. State Univ., San Jose. 88 p.

- Speer P. E. and D. J. Aubrey. 1985. A study of non-linear tidal propagation in shallow inlet/estuarine systems Part II: Theory. Estuarine, Coastal and Shelf Science. 21:207-224.
- Sternberg, R. W. 1967. Measurements of Sediment Movement and Ripple Migration in a Shallow Marine Environment. Marine Geology. 5:195-205.
- Sverdrup, H. U., M. W. Johnson and R. H. Fleming 1942. The Oceans. Their Physics, Chemistry, and General Biology. Prentice Hall. New York, N. Y. 1087 p.
- Water Resource Engineers. 1968. Investigation to develop a water quality control plan for Moss Landing Harbor and Elkhorn Slough, Monterey County. 63 p.

APPENDIX 1

Current meter characteristics and calibrations

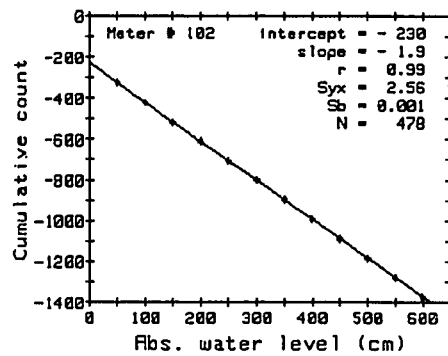
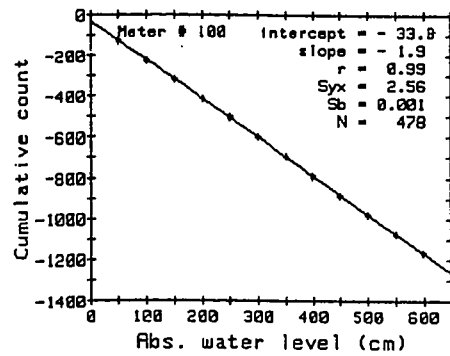
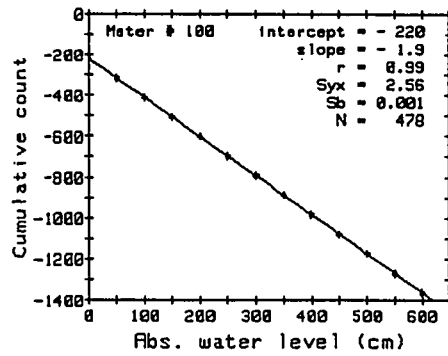
APPENDIX 1 Current meter characteristics

	Endeco	S4
Current Speed		
Sensitivity	57.58 RPM/51.44cm/s	
Range	0 to 223.2 cm/s @ 2 min interval	0 to 350 cm/s @ 2 min interval
Threshold	< 2.57 cm/s	< 1.0 cm/s
Resolution	0.9 cm/s	0.2 cm/s
Accuracy	± 3.0 % (full scale)	± 2.0 % (full scale)
Current Direction		
Range	360°	360°
Resolution	1.4°	0.5°
Accuracy	± 7.2°	± 2.0°
Temperature		
Sensor	Thermistor	Semiconductor
Range	-5 to +45 °C	-5 to +45 °C
Resolution	0.2 °C	0.2 °C
Accuracy	± 0.1 °C	± 0.05 °C
Depth	(Kavilco transducer)	
Range	11 m	0 to 1000 dBar (station 1) 0 to 70 dBar (station 2)
Resolution	0.5 cm	1 dBar (1000 dBar) 4 mm (70 dBar)
Accuracy	± 2.5 cm	± 0.25 % (full scale)

Algorithm for Kavilco P650 pressure transducer

$$\begin{aligned}
 P_{100} &= [(N - 221) - (256 * M)] * 0.52 \\
 P_{101} &= [(N - 33.8) - (256 * M)] * 0.53 \\
 P_{102} &= [(N - 230) - (256 * M)] * 0.53
 \end{aligned}$$

where P is water depth, N is observed pressure counts and M is the number of foldover ranges. The depth range before folding occurs is 1.3 m.



Calibration curves for Kavalco pressure transducers

APPENDIX 2

Tidal Constituents

Appendix 2

TIDAL CONSTITUENTS

Station # 483: Monterey, California
 Latitude 36 36.3 N Longitude 121 53.3 W
 20 Constituents from Analysis of 365 Day Series in 1974

#	Name	Speed # deg/hr	Amplitude ft	Kappa deg	hrs
0	MSL		2.870		
1	J1	15.585443	0.071	107.0	6.9
2	K1	15.041069	1.216	97.8	6.5
3	K2	30.082137	0.121	287.7	9.6
4	L2	29.528479	0.046	322.8	10.9
5	M1	14.496694	0.117	114.8	7.9
6	M2	28.984104	1.628	297.4	10.3
11	N2	28.439730	0.366	272.0	9.6
12	2N2	27.895355	0.046	248.5	8.9
13	O1	13.943036	0.763	81.4	5.8
14	OO1	16.139102	0.039	119.6	7.4
15	P1	14.958931	0.381	92.7	6.2
16	Q1	13.398661	0.137	72.9	5.4
17	2Q1	12.854286	0.020	65.0	5.1
19	S1	15.000000	0.038	202.3	13.5
20	S2	30.000000	0.425	295.5	9.9
23	T2	29.958933	0.025	295.5	9.9
24	lmbda2	29.455625	0.011	296.5	10.1
25	mu2	27.968208	0.046	234.4	8.4
26	nu2	28.512583	0.069	279.4	9.8
27	rho1	13.471515	0.029	74.3	5.5

Extreme Tides: Low = -2.7 High = 8.5
 Principle Range $2*(K1+O1+M2+S2)$ = 4.0
 Form Ratio $(K1+O1)/(M2+S2)$ = 0.96

Appendix 2 (cont.).

TIDAL CONSTITUENTS

Station # 485: Moss Landing, California

Latitude 36 48.1 N Longitude 121 47.4 W

20 Constituents from Analysis of 29 Day Series in 1976

#	Name	Speed # deg/hr	Amplitude ft	Kappa deg	hrs
0	MSL		2.790		
1	J1	15.585443	0.058	108.0	6.9
2	K1	15.041069	1.135	99.3	6.6
3	K2	30.082137	0.114	295.8	9.8
4	L2	29.528479	0.047	321.2	10.9
5	M1	14.496694	0.052	90.6	6.2
6	M2	28.984104	1.664	295.3	10.2
11	N2	28.439730	0.342	269.5	9.5
12	2N2	27.895355	0.046	243.7	8.7
13	O1	13.943036	0.728	81.8	5.9
14	OO1	16.139102	0.031	116.7	7.2
15	P1	14.958931	0.378	99.3	6.6
16	Q1	13.398661	0.141	73.1	5.5
17	2Q1	12.854286	0.019	64.3	5.0
18	R2	30.041067	0.003	295.8	9.8
20	S2	30.000000	0.418	295.8	9.9
23	T2	29.958933	0.025	295.8	9.9
24	1mbda2	29.455625	0.012	295.5	10.0
25	mu2	27.968208	0.040	294.8	10.5
26	nu2	28.512583	0.066	273.0	9.6
27	rho1	13.471515	0.028	74.3	5.5

Extreme Tides: Low = -2.6 High = 8.1
 Principle Range $2*(K1+O1+M2+S2)$ = 3.9
 Form Ratio $(K1+O1)/(M2+S2)$ = 0.89

Appendix 2 (cont.)

TIDAL CONSTITUENTS

Station # 493: Elkhorn Slough, California

Latitude 36 49.1 N Longitude 121 44.7 W

22 Constituents from Analysis of 365 Day Series in 1976

#	Name	Speed # deg/hr	Amplitude ft	Kappa deg	hrs
0	MSL		2.760		
1	J1	15.585443	0.062	130.9	8.4
2	K1	15.041069	1.168	103.0	6.8
3	K2	30.082137	0.119	283.9	9.4
4	L2	29.528479	0.031	297.7	10.1
5	M1	14.496694	0.047	130.8	9.0
6	M2	28.984104	1.630	303.7	10.5
8	M4	57.968208	0.044	356.5	6.1
11	N2	28.439730	0.370	280.3	9.9
12	2N2	27.895355	0.044	255.1	9.1
13	O1	13.943036	0.725	87.1	6.2
14	OO1	16.139102	0.036	147.3	9.1
15	P1	14.958931	0.377	100.8	6.7
16	Q1	13.398661	0.129	82.1	6.1
17	2Q1	12.854286	0.019	71.2	5.5
18	R2	30.041067	0.003	306.3	10.2
20	S2	30.000000	0.426	306.3	10.2
23	T2	29.958933	0.025	306.3	10.2
24	1mbda2	29.455625	0.011	304.9	10.4
26	nu2	28.512583	0.062	286.4	10.0
27	rho1	13.471515	0.028	80.3	6.0
28	MK3	44.025173	0.050	185.4	4.2
29	2MK3	42.927140	0.044	196.2	4.6

Extreme Tides: Low = -2.7 High = 8.2
 Principle Range $2*(K1+O1+M2+S2)$ = 3.9
 Form Ratio $(K1+O1)/(M2+S2)$ = 0.92